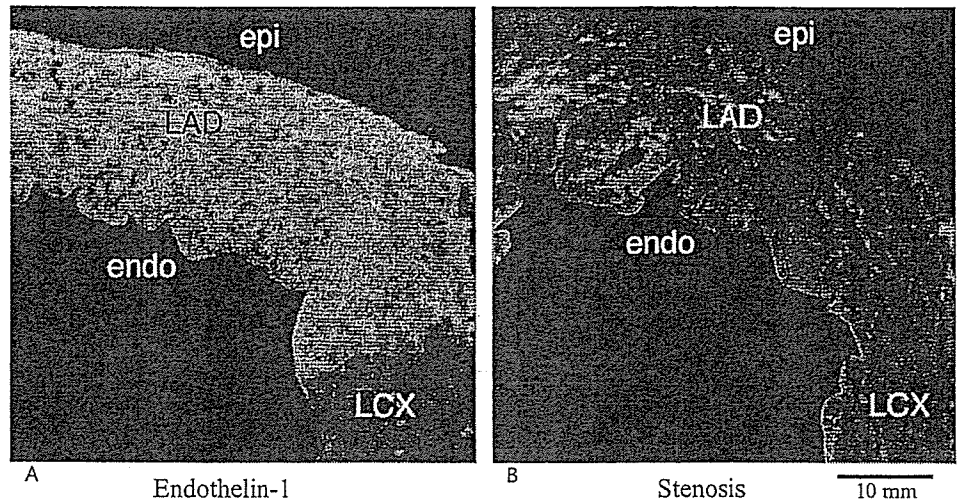

FIGURE 1. NADH fluorescence photographs of cross-sectional frozen heart slices. The slices show short-axial view at mid-left ventricle. LAD, left anterior descending coronary artery perfused myocardium; LCX, left circumflex coronary artery perfused myocardium; Epi, Epicardial side; Endo, Endocardial side. A, Endothelin-1 decreased coronary inflow by 36% and produced a transmural extension of positive NADH fluorescence. B, Stenosis reduced coronary inflow by 32% and produced positive NADH fluorescence (ischemia) in the subendocardium.

Chemical Analyses of Tissue Metabolites

The higher NADH content as well as the lower NAD/NADH ratio in both the subepicardial and the subendocardial layers of the ischemic LAD areas in the endothelin group indicated more severe anaerobic metabolism than in the stenosis group (Table 3). These indicators are the most sensitive marker of the redox states in ischemic myocardium; no difference in classic ischemic markers like lactate, ATP, or CP were observed between the two treatment groups (Table 3).

In NADH-fluorescent myocardium, the NADH concentrations were significantly higher than those in NADH-non-fluorescent areas (0.77 ± 0.20 versus 0.40 ± 0.08 nmol/mg, n = 27, and 33, respectively, $P < 0.0001$). This result confirmed the strong link between positive NADH fluorescence and the anaerobic state in frozen heart samples.

Protocol 2

Regional Coronary Blood Flow

In a preliminary study, the injection of microspheres (more than 1×10^4/g) into canine hearts to measure myocardial flow was shown to produce microspots of NADH fluorescence caused by microsphere embolization-induced ischemia,[22] indicating that the concomitant measurement of tissue flow in the hearts of animals treated with protocol 1 could not be accurately evaluated (Table 4). Therefore, we performed a separate but parallel protocol of NADH fluorescence study to analyze myocardial tissue flow using the microsphere method. The heart rates and mean aortic pressures were comparable with those in protocol 1 and did not change significantly throughout the experiment. Coronary inflow reductions were also comparable with those in protocol 1 (29.4 ± 5.2% in the endothelin group, and 30.0 ± 2.7% in the stenosis group, ns). Flow in myocardial tissue and the flow ratio in endo/epi tissues were not significantly reduced in either group, although the calculated subepicardial coronary vascular resistance was higher in the endothelin group than in the stenosis group. Neither the absolute flow value nor the endo/epi flow ratio were able to account for the larger ischemic areas observed in the endothelin group in protocol 1.

DISCUSSION

Endothelin-1 directly constricts coronary smooth muscle and decreases blood flow, leading to severe myocardial ischemia; however the effects of ET-1 on myocardial ischemia in vivo have not been well characterized. This study produced the following findings: (1) ET-1 enlarged the myocardial ischemic area detected by NADH fluorescence, compared with that induced by similar reduction in coronary flow arising from stenosis. Moreover, ET-1 decreased the NAD/NADH ratio in both the subendocardium and the subepicardium, compared with the situation in the stenosis group, suggesting that ET-1 has flow-independent, direct pro-ischemic effects on myocytes in vivo. (2) ET-1 increased the coronary vascular resistance dominantly in the subepicardium and increased the ischemic area and the NADH content in the same region. These data suggest that ET-1 more selectively constricts subepicardial arterioles, extends myocardial ischemia transmurally, and causes an ST-elevation. (3) ET-1 generated smaller ischemic foci in the microcirculation than those generated by stenosis,

TABLE 2. Quantification of Ischemic Area and Transmural Distribution

	Endothelin Group (n = 8)			Stenosis Group (n = 7)			Endothelin vs. Stenosis	
	Endo Mean (SD)	Epi Mean (SD)	Statistics	Endo Mean (SD)	Epi Mean (SD)	Statistics	Endo	Epi
Ischemic area								
Endo or epi (%)	66.3 (22.3)	66.8 (23.3)	ns	27.7 (27.2)	8.5 (10.3)	$P = 0.03$	$P = 0.01$	$P < 0.0001$
Total (%)	66.4 (22.5)			17.6 (18.2)			$P = 0.0005$	

© 2005 Lippincott Williams & Wilkins

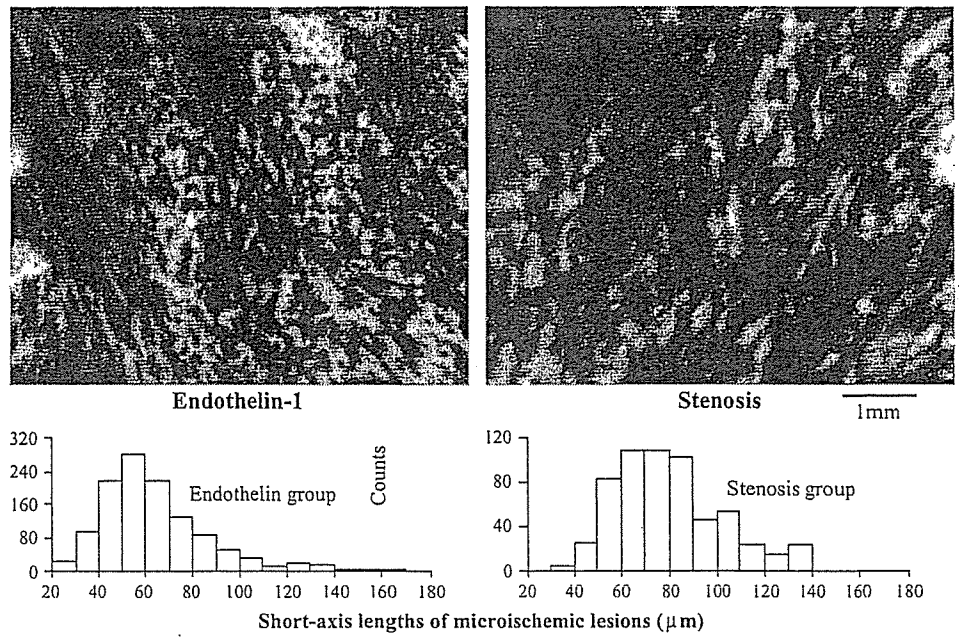

FIGURE 2. Magnified NADH fluorescence photographs (×100) showing microischemic foci in both the endothelin and stenosis groups. The histogram shows the distributions of the short-axis lengths of microischemic lesions in both groups. The endothelin group produced many similar shaped but smaller ischemic foci, compared with the stenosis group (61 ± 18 versus 76 ± 18 μm, $P < 0.0001$).

suggesting that the distal arteriolar levels of the coronary microcirculation may be affected by ET-1.

We found a clear dissociation between the reduction of coronary blood flow and the development of myocardial ischemia in the endothelin group, compared with the situation in the stenosis group. This finding was especially noticeable in the subendocardial region. In the endothelin group, we observed a subendocardial blood flow similar to that in the stenosis group, as detected using the non-radioisotope microsphere method. However, the ischemic area detected by NADH fluorescent was larger by more than two fold. This data clearly shows the flow-independent pro-ischemic effects of ET-1 in vivo. Although we did not clarify the direct mechanism of the pro-ischemic effects of ET-1 on myocytes, ET-1 may increase the oxygen demand of the myocytes. Previous reports have shown that endothelin-1 can increase intracellular Ca^{2+} through the activation of voltage-dependent Ca^{2+} currents[23,24] and can activate Na^{+}-H^{+} exchange on isolated myocytes,[25] both of which produce inotropic effects and augment oxygen demand.[10,11] An increased left ventricular dP/dt following the intravenous administration of endothelin-1 was also reported in canine and rat model.[9,26] Furthermore, using an ex vivo Langendorff model of rat hearts, Grover et al[27] demonstrated the extension of myocardial ischemia in arrested heart, suggesting the pro-ischemic effect of endothelin-1. ET-1 was also reported to augment myocardial mitochondrial damage induced by rotenone; therefore, mitochondrial dysfunction during ischemia may also be enhanced by ET-1.[28] ET-1 can elicit the positive-inotropic effects by the cross-talk with norepinephrine and a release of norepinephrine in the operation may enhance the pro-ischemic effects of ET-1.[29] In this study, ET-1 did not change the heart rate or the myocardial ATP content; however, we speculate that positive inotropic effects associated with an enhanced metabolic demand or an aggravation of mitochondrial dysfunction may cause the pro-ischemic effects of ET-1.

Another interesting finding was the difference in the distribution of myocardial ischemia between the endothelin and stenosis groups. In the coronary stenosis group, both the reduction of tissue flow and the distribution of ischemia were

TABLE 3. Chemical Analyses of Myocardial Microsampling of Subendocardial or Subepicardial Layer in the Endothelin and Stenosis Groups

	Endothelin Group			Stenosis Group			Endothelin vs. Stenosis	
	Endo Mean (SD)	Epi Mean (SD)	Statistics	Endo Mean (SD)	Epi Mean (SD)	Statistics	Endo	Epi
	n = 17	n = 17		n = 14	n = 14			
NADH (nmol/mg)	0.68 (0.25)	0.67 (0.27)	ns	0.5 (0.22)	0.39 (0.08)	ns	$P = 0.048$	$P = 0.001$
NAD/NADH	7.4 (2.9)	7.6 (3.5)	ns	10.9 (5.0)	12.5 (2.6)	ns	$P = 0.02$	$P = 0.0001$
Lactate (nmol/mg)	26.0 (12.9)	28.8 (13.9)	ns	31.0 (10.5)	22.9 (8.5)	$P = 0.04$	ns	ns
ATP (nmol/mg)	42.8 (8.5)	45.1 (11.1)	ns	43.0 (6.9)	41.7 (9.2)	ns	ns	ns
CP (nmol/mg)	67.3 (27.7)	74.7 (30.9)	ns	63.4 (11.7)	72.5 (20.3)	ns	ns	ns

ATP, adenosine triphosphate; CP, creatine phosphate.

© 2005 Lippincott Williams & Wilkins

TABLE 4. Tissue Flow and Hemodynamics in the Stenosis and Endothelin Groups

	Control Group Mean (SD)	Stenosis Group Mean (SD)	Endothelin Group Mean (SD)	ANOVA
CVR (mm Hg/mL/min/g)				
Endo	134 (48)	100 (35)	161 (90)	ns
Epi	118 (56)	67* (16)	160* (86)	$P = 0.03$
Tissue flow (mL/min/g)				
Endo	0.93 (0.29)	0.71 (0.23)	0.97 (0.53)	ns
Epi	1.14 (0.43)	1.01 (0.27)	0.86 (0.31)	ns
Heart rate (/min)	180 (13)	180 (12)	181 (13)	Ns
mAOP (mm Hg)	115 (15)	115 (15)	117 (14)	Ns
mCPP (mm Hg)	117† (13)	65†‡ (13)	119‡ (15)	$P < 0.0001$

CVR, coronary vascular resistance; mAOP, mean aortic pressure; mCPP, mean coronary perfusion pressure (n = 7).
*Stenosis group vs. endothelin group: $P = 0.0093$; †Control group vs. stenosis group: $P < 0.0001$; ‡Stenosis group vs. endothelin group: $P < 0.0001$.

predominant in the subendocardium. ET-1 administration, however, significantly increased the subepicardial coronary vascular resistance. The increase in the ST-elevation by ET-1 could be due to the transmural development of myocardial ischemia, because subepicardial ischemia widens the solid angle of the subepicardial electrode toward the ischemia front, resulting in an increase in the ST-segment.[30] A decrease in subepicardial blood flow induced by ET-1 was also reported by Clozel[31] and Ricou.[32] Although the precise mechanism for the change in the coronary flow distribution induced by ET-1 remains unclear, differences in the transmural distributions or affinities of the ET-1 receptor or the target molecules of ET-1 (for example, ATP-sensitive potassium channels) may explain this interesting phenomenon.[33,34]

Karwatovska-Prokopczuk et al[5] challenged the comparison of endothelin-induced and mechanically induced flow reductions in Langendorff-perfused rabbit hearts, claiming that ET-1 did not exacerbate ischemia. They assessed myocardial ischemia by evaluating oxygen consumption, pH, and purine bodies in the coronary sinus blood. We observed the selective vasoconstriction in the subepicardium using NADH fluorescence; therefore, it might be difficult to assess myocardial ischemia by examining coronary sinus blood. We also tried to measure arterio-venous differences in oxygen and lactate in the coronary circulation but could not identify any ischemia severity between the two treatment groups (data not shown). We also found that some indicators of myocardial ischemia, such as the lactate or creatine phosphate content, were similar in the two treatment groups. Because an increase in NADH and a decrease in the NAD/NADH ratio are the most rapid and sensitive markers for the ischemic redox changes, the method used in the present study can clarify the extent and severity of metabolic changes with a higher sensitivity.

The third unique effect of ET-1 was the appearance of making smaller ischemic foci in the microcirculation, compared with these observations in the stenosis model, as detected by the visualization of many spindle-shaped microischemic foci. Because ET-1 constricts more distal arterioles, as reported by microscopic observation of narrowing small vessels, ET-1 can dominantly regulate coronary microcirculation.[35,36] Under the low flow condition induced by stenosis, subepicardial arteries are maximally dilated, preventing the extension of ischemia. However, the systolic compression of subendocardial arteries limits this compensatory mechanism and induces subendocardial ischemia. A similar size of microischemia was observed in a hemorrhagic shock model.[22]

CONCLUSION

Endothelin-1 produced a larger ischemic area than stenosis in the presence of equivalent reduction in coronary inflow. The mechanism for ET-1–induced ischemia might depend on direct pro-ischemic effects on myocytes and vasoconstriction of the coronary microcirculation, predominantly in the subepicardium in vivo.

ACKNOWLEDGMENTS

The authors thank Mr. Yozo Ohnishi in the Faculty of Medical Equipment of Keio University for his dedicated and excellent technical support and Dr. Motoaki Bessho of the Eisai Tokyo Laboratory for his excellent support in analysis of the metabolites in the myocardial tissues. We also appreciate Mr. Wataru Kawamura of Karl Zeiss Vision Co. Ltd. for his support in analyzing the size of the microischemic foci.

REFERENCES

1. Yanagisawa M, Kurihara H, Kimura S, et al. A novel potent vasoconstrictor peptide produced by vascular endothelial cells. *Nature*. 1988;232:411–415.
2. Igarashi Y, Aizawa Y, Tamura M, et al. Vasoconstrictor effect of endothelin on the canine coronary artery: Is a novel endogenous peptide involved in regulating myocardial blood flow and coronary spasm. *Am Heart J*. 1989;118:674–678.
3. Vojacek J, Kolar J, Lisy O, et al. Time course of endothelin-1 plasma level in patients with acute coronary syndromes. *Cardiology*. 1999;91:114–118.
4. Muramatsu K, Tomoike H, Ohara Y, et al. Effects of endothelin-1 on epicardial coronary tone, coronary blood flow, ECG-ST change and regional wall motion in anesthetized dogs. *Heart Vessels*. 1991;6:191–196.
5. Karwatowska-Prokopczuk E, Wennmalm Å. Effects of endothelin on coronary flow, and mechanical performance, oxygen uptake, and formation of purines and on outflow of prostacyclin in the isolated rabbit heart. *Circ Res*. 1990;66:46–54.
6. Fukuda K, Hori S, Kusuhara M, et al. Intracoronary endothelin-1 increases coronary retrograde pressure by constricting arterioles. *Cardiovasc Res*. 1990;24:987–992.

© 2005 Lippincott Williams & Wilkins

7. Watanabe T, Suzuki N, Shimamoto N, et al. Endothelin in myocardial infarction. *Nature*. 1990;344:114.
8. Grover GJ, Dzwonczyk S, Parham CS. The endothelin-1 receptor antagonist BQ-123 reduces infarct size in a canine model of coronary occlusion and reperfusion. *Cardiovasc Res*. 1993;27:1613–1618.
9. Kitayoshi T, Watanabe T, Shimamoto N. Cardiovascular effects of endothelin in dogs: positive inotropic action in vivo. *Eur J Pharmacol*. 1989;166:519–522.
10. Ishikawa T, Yanagisawa M, Kimura S, et al. Positive inotropic action of novel vasoconstrictor peptide endothelin on guinea pig atria. *Am J Physiol*. 1988;255:H970–H973.
11. Takahashi M, Endoh M. Characterization of positive inotropic effect of endothelin on mammalian ventricular myocardium. *Am J Physiol*. 1991; 261:H611–H619.
12. Maczewski M, Beresewicz A. The role of endothelin, protein kinase C and free radicals in the mechanism of the post-ischemic endothelial dysfunction in guinea-pig hearts. *J Mol Cell Cardiol*. 2000;32:297–310.
13. Bessho M, Tajima T, Hori S, et al. NAD and NADH values in rapidly sampled dog heart tissues by two different extraction methods. *Anal Biochem*. 1989;182:304–308.
14. Hori S, Nakazawa H, Ohnishi Y, et al. A rapid cross-sectioning and freeze-clamping device for the beating canine heart. *J Mol Cell Cardiol*. 1989;21: 203–210.
15. Kurihara H, Yamaoki K, Nagai R, et al. Endothelin: a potent vasoconstrictor associated with coronary vasospasm. *Life Sci*. 1989;44: 1937–1943.
16. Barlow CD, Chance B. Ischemic areas in perfused rat heart: measured by NADH fluorescence photography. *Science*. 1976;193:909–910.
17. Chance B, Williamson JR, Jamieson D, et al. Properties and kinetics of reduced pyridine nucleotide fluorescence of the isolated and in vivo rat heart. *Biochem Z*. 1965;341:357–377.
18. Karp MT, Rauniop RP, Lovgren TN-E. Simultaneous extraction and combined bioluminescent assay of NAD+ and NADH. *Anal Biochem*. 1983;128:175–180.
19. Shimojo N, Naka K, Nakajima C, et al. Test-strip method for measuring lactate in whole blood. *Clin Chem*. 1989;35:1992–1994.
20. Lowry OH, Rosebrough NJ, Farr AL. Protein measurement with the Folin phenol reagent. *J Biochem*. 1951;193:265–275.
21. Mori H, Haruyama S, Shinozaki Y, et al. New nonradioactive microspheres and more sensitive X-ray fluorescence to measure regional blood flow. *Am J Physiol*. 1992;263:H1946–H1957.
22. Miyazaki K, Hori S, Inoue S, et al. Characterization of energy metabolism and blood flow distribution in myocardial ischemia in hemorrhagic shock. *Am J Physiol*. 1997;273:H600–H607.
23. Xu Y, Sandirasegarane L, Gopalakrishnan V. Protein kinase C inhibitors enhance endothelin-1and attenuate vasopressin and angiotensin II evoked [Ca2+] i elevation in the rat cardiomyocyte. *Br J Pharmacol*. 1993;108: 6–8.
24. Lauer MR, Gunn MD, Clusin WT. Endothelin activates voltage dependent Ca2+ current by a G protein-dependent mechanism in rabbit cardiac myocytes. *J Physiol*. 1992;448:729–747.
25. Khandoudi N, Ho J, Karamazyn M. Role of Na+-H+ exchange in mediating effects of endothelin-1 on normal and ischemic/reperfused hearts. *Circ Res*. 1994;75:369–378.
26. Beyer ME, Slesak G, Nerz S, et al. Effects of endothelin-1 and URL 1620 on myocardial contractility and myocardial energy metabolism. *J Cardiovasc Pharmacol*. 1995;26(Suppl 3):S150–S152.
27. Grover GJ, Sleph PG, Fox M, et al. Role of endothelin-1 and big endothelin-1 in modulating coronary vascular tone, contractile function and severity of ischemia in rat hearts. *J Pharmacol Exp Ther*. 1992;263: 1074–1082.
28. Yuki K, Suzuki T, Katoh S, et al. Endothelin-1 stimulates cardiomyocyte injury during mitochondrial dysfunction in culture. *Eur J Pharmacol*. 2001;431:163–170.
29. Chu L, Takahashi R, Norota I, et al. Signal transduction and Ca2+ signaling in contractile regulation induced by crosstalk between endothelin-1 and norepinephrine in dog ventricular myocardium. *Circ Res*. 2003;92:1024–1032.
30. Holland RP, Arnsdorf MF. Solid angle theory and the electrocardiogram: physiologic and quantitative interpretations. *Prog Cardiovasc Dis*. 1977; 19:431–457.
31. Clozel JP, Clozel M. Effect of endothelin on the coronary vascular bed in open-chest dogs. *Circ Res*. 1989;65:1193–1200.
32. Ricou FJ, Murata K, Oh B-H, et al. Evaluation of inotropic effect of endothelin-1 in vivo. *J Cardiovasc Pharmacol*. 1992;20:671–677.
33. Furukawa T, Kimura S, Furukawa N, et al. Role of cardiac ATP-regulated potassium channels in differential responses of endocardial and epicardial cells to ischemia. *Circ Res*. 1991;68:1693–1702.
34. Miyoshi Y, Nakaya Y, Wakatsuki T, et al. Endothelin blocks ATP-sensitive K+ channels and depolarizes smooth muscle cells of porcine coronary artery. *Circ Res*. 1992;70:612–616.
35. Marcus M, Chilian WM, Kanatsuka H, et al. Understanding the coronary circulation through studies at the microvascular level. *Circulation*. 1990; 82:1–7.
36. Wan W, Kanatsuka H, Akai K, et al. Effects of low doses of endothelin-1 on basal vascular tone and autoregulatory vasodilatation in canine coronary microcirculation in vivo. *Jpn Circ*. 1999;63:617–623.

© 2005 Lippincott Williams & Wilkins

Molecular and Cellular Biochemistry **268:** 59–66, 2005.
© 2005 *Kluwer Academic Publishers. Printed in the Netherlands.*

Cardiac syntrophin isoforms: Species-dependent expression, association with dystrophin complex and subcellular localization

Yuko Iwata,[1] Munekazu Shigekawa[2] and Shigeo Wakabayashi[1]

[1]*Department of Molecular Physiology, National Cardiovascular Center Research Institute, Fujishiro-dai, Suita, Osaka, Japan;* [2]*Department of Human Life Sciences, Senri Kinran University, Suita, Osaka, Japan*

Received 27 May 2004; accepted 24 June 2004

Abstract

Syntrophin is known to be a component of the dystrophin-glycoprotein complex (DGC), a membrane/cytoskeleton-anchoring structure that is essential for the maintenance of viability of sarcolemma. We purified DGC from hearts of human and several animal species, and compared their protein composition. While almost all components of DGC were present in various species, proteins with the apparent molecular mass of 50–65 kDa corresponding to syntrophin isoforms were very different among them. Three isoforms of syntrophin ($\alpha 1$, $\beta 1$, $\beta 2$) were expressed in hamster, rat and canine ventricles, whereas only $\alpha 1$-isoform was mainly expressed in human and rabbit ventricles. Immunohistochemical analysis revealed that $\alpha 1$-and $\beta 2$-syntrophins were co-localized in sarcolemma and in T-tubules of canine ventricles. However, despite membrane localization of most syntrophins, subcellular fractionation revealed that part of syntrophins were recovered in the cytosolic fraction devoid of other components of DGC, raising the possibility that syntrophins may play multiple roles in various intracellular sites of cardiac muscle cells. Species-dependent expression and unique subcellular localization of syntrophins in cardiac muscle may contribute to the variable severity of muscle dysgenesis caused by the same primary defect in components of DGC of human and other animal species. (Mol Cell Biochem **268:** 59–66, 2005)

Key words: cardiac muscle, syntrophin, dystrophin, dystrophin-associated proteins, subcellular localization

Abbreviation: DGC – dystrophin–glycoprotein complex, DAP – dystrophin-associated protein, SG – sarcoglycan, DG – dystroglycan, WGA – wheat germ agglutinin, NAG – N-acetyl glucosamine, CBB – Coomassie brilliant blue, DTT – dithiothreitol, PMSF – phenylmethylsulfonyl fluoride, MBP – maltose binding protein, GST – glutathione S-transferase, SDS-PAGE – sodium dodecyl sulfate-polyacrylamide gel electrophoresis

Introduction

Mutations in several components of the dystrophin-glycoprotein complex (DGC) are known to be involved in the pathogenesis of muscular dystrophies including cardiomyopathy. Previous studies suggested that the severity of muscle dysgenesis caused by the primary defect in components of DGC is dependent on the muscle-type and species. For example, in Duchenne muscular dystrophy, a minority of patients die of cardiac failure, although cardiac dysfunction occurs very frequently in these patients [1]. In *mdx* mouse, in which dystrophin is totally deficient in both cardiac and skeletal muscle, dysfunction of cardiac muscle is usually absent [2]. In contrast, most patients with X-linked cardiomyopathy, in which the primary defect occurs presumably in the same dystrophin gene, have a rapidly progressive myocardial

Address for offprints: Y. Iwata, Department of Molecular Physiology, National Cardiovascular Center Research Institute, Fujishiro-dai 5-7-1, Suita, Osaka 565, Japan (E-mail: yukoiwat@ri.ncvc.go.jp)

disorder without clinical signs of skeletal myopathy [3]. Patients having skeletal muscle myopathy with variable severity due to mutation in the α-sarcoglycan (SG) gene are mostly free from heart dysfunction [4]. On the other hand, in the cardiomyopathic Syrian hamster, an animal model for the δ-SG deficiency [5] and also a model for the hereditary human cardiomyopathy, the animal usually dies mostly of heart failure, not of respiratory failure. Furthermore, it is known that a C-terminal transcript of the dystrophin gene that is not present in skeletal muscle is present in cardiac muscle [6]. All these observations raised the possibility that there is some biochemical and functional difference among animal species or muscle-type. However, at present very little information is available on DGC and its distribution in human cardiomyocytes because few studies [7–10] have been done on dystrophin and DAP in cardiac muscle.

Syntrophin is known to be an important component of DGC, a membrane/cytoskeletal-anchoring structure that is essential for the maintenance of viability of sarcolemma. To date five syntrophin isoforms $\alpha 1$, $\beta 1$, $\beta 2$, $\gamma 1$, $\gamma 2$ have been identified [11, 12]). Of these isoforms, $\alpha 1$, $\beta 1$, $\beta 2$-syntrophins are known to be expressed in striated muscles [11]. On the other hand, $\gamma 1$-syntrophin is expressed uniquely in the brain, whereas $\gamma 2$-syntrophin has a somewhat broader distribution [12]. Each syntrophin is encoded by a separate gene but shares a common domain organization and contains two tandem pleckstrin homology domains at the amino-terminus, a single PDZ domain, and a highly conserved carboxyl-terminal syntrophin-unique region [11, 12], predicting multiple roles in anchoring proteins at the membrane through the PDZ domain and in signal transduction. We previously reported that the protein composition of the hamster cardiac DGC was significantly different from the rabbit skeletal DGC, and that amount of proteins in DGC was five times more abundant in cardiac than in skeletal muscle [13]. These differences of DGC components between skeletal and cardiac muscles or among animal species may explain the difference observed as for the above-mentioned severity of dysgenesis of these muscles.

In this study, we purified the DGC from human ventricular muscle and compared its components with those isolated from hamster, rabbit, and canine cardiac muscles, and found that in cardiac muscle the expression pattern of syntrophin isoforms is different among species. In addition, we studied on subcellular localization of syntrophin isoforms in cardiac muscle.

Materials and methods

Purification of dystrophin-DAP complex

Human samples were obtained at an autopsy from patients without heart disease. Frozen ventricles (5 g) were homogenized for 30 s three times with Physcotron NS-10 at 25,000 rpm in 50 ml buffer A (1% digitonin, 0.5 M NaCl, 50 mM Tris-HCl (pH 7.4), 1.5 mM benzamidine, 0.25 mM PMSF, 2.5 ng/ml leupeptin, 2.5 ng/ml pepstatin A, and 2.5 ng/ml aprotinin). After centrifugation at 100, $000 \times g$, the supernatant was incubated overnight at 4 °C with 40 ml of 50% slurry of succinylated WGA-agarose beads (Vector Laboratories, Burlingane, CA, USA) [13, 14]. The beads were washed extensively with 400 ml buffer B (the same composition as buffer A except for a reduced concentration of digitonin (0.1%)) and then eluted with 120 ml buffer B containing 0.35 M NAG. The eluate was diluted 10-fold with buffer C (buffer B without NaCl) and applied to a DEAE-cellulose (10 ml) column. The column was then eluted stepwise with buffer C containing following NaCl concentrations; 110 mM (300 ml), 175 mM (300 ml), 250 mM (100 ml), and 500 mM (100 ml). The dystrophin-DAP complex was also purified in the same way from the frozen hamster, rabbit and canine heart. Experimental procedures on human subjects were followed in accordance with the ethical standards of the responsible committee on institutional human experimentation. The care and use of laboratory animals were followed by the institution's guide.

Antibody production

We raised mouse monoclonal antibody anti-pan-syntrophin against syntrophin using the fraction eluted from succinylated WGA at 0.35 M NAG (see above) as antigens by the method described previously [13]. This antibody recognized all three isoforms of syntrophin because it reacted against PDZ domain of syntrophin. We raised isoform specific polyclonal antibodies by immunizing rabbits with peptide according to standard methods [14]. The anti-$\alpha 1$-syn and anti-$\beta 1$-syn were prepared against the peptide RQPSSPGPQPRNLSEA ($\alpha 1$) and DPPSSQSFSFHRDR ($\beta 1$) corresponding to amino acids of human $\alpha 1$-syntrophin and human $\beta 1$-syntrophin [1]. Monoclonal antibody against $\beta 2$-syntrophin was raised by immunizing mouse with glutathion-S-transferase (GST) fusion protein containing $\beta 2$ specific domain of mouse $\beta 2$-syntrophin (aa 175–271). Affinity purification of antibodies was performed as described previously [13].

The isoform specificity of these polyclonal and monoclonal antibodies was verified by immunoblot analysis using mouse and hamster tissues (Fig. 3, [15]). Purified antibodies (anti-pan-syntrophin and anti-$\alpha 1$-syn) were coupled to activated aldehyde on agarose (Actigel, Sterogene, CA, USA) to prepare immunoaffinity adsorbents. We used mouse monoclonal antibody M156 against hamster α-dystroglycan (DG) and rabbit polyclonal antibodies p50 and p43 against rabbit α-SG and β-DG as described previously [13]. Polyclonal chicken antibody against GST fusion protein containing aa 1-291 of hamster γ-sarcoglycan was prepared

as described previously. These polyclonal antibodies were subsequently affinity purified as described previously [16]. We purchased mouse monoclonal antibodies NCL-Dysl and NCL-Dys2 raised against the rod portion (aa 1181–1388) and C-terminus (aa 3669–3685) of human dystrophin and mouse monoclonal antibodies NCL-DRP2 and NCL-DRP1 raised against the N-terminal domain (first 261 amino acids) and C-terminus (last 11 amino acids) of human utrophin and mouse monoclonal antibodies NCL-β-SARC raised against the fusion protein of the human β-SG sequence and NCL-δ-SARC raised against N-terminus (first 19 amino acids) peptide of human δ-SG (Novocastle Laboratories, Newcasle, UK). Mouse monoclonal antibody mab SYN1351 raised against *Torpedo* syntrophin [17] was a gift from Dr. Stanley C. Froehner.

Preparation of cytosolic and membrane fractions

Ventricular muscles (1 g) from normal and BIO 14.6 hamsters and human were homogenized in 1 ml of 10 mM NaHCOs or containing 0.5 M NaCl medium for 30 s three times and centrifuged at 5500 $\times$ g (max). The low spin supernatants were further centrifuged at 480,000 $\times$ g (max) for 40 min. Aliquots of low spin supernatants (total) and high spin supernatant (cytosolic fraction) and high spin precipitant (membrane fraction) were subjected to SDS-PAGE. Proteins were blotted to Immobilon membranes and then immunostained with anti-dystrophin, anti-pan-syntrophin and anti-β-DG antibodies respectively. (1; total, 2; cytosolic fraction, 3, membrane fraction Fig. 6A).

Other procedures

Quantitative immunoblot analysis [14] and immunocytochemistry [18] and immunoprecipitation [18] were performed as described previously. Protein concentration was measured using a bicinchoninic acid assay system (Pierce Chemical, Rockford, USA) with bovine serum albumin as a standard.

Results

Purification of human cardiac DGC

In this study, we developed the method to purify DGC from a limited amount of human heart tissues. An important step for purification is that the ventricle is directly homogenized in the presence of 1% digitonin and subjected to next chromatography steps. We found that about 60% of dystrophin in the ventricular muscle was extracted into the supernatant in the initial homogenization step. The eluate from DEAE-cellulose was enriched in dystrophin (Mr. 400 kDa) and other

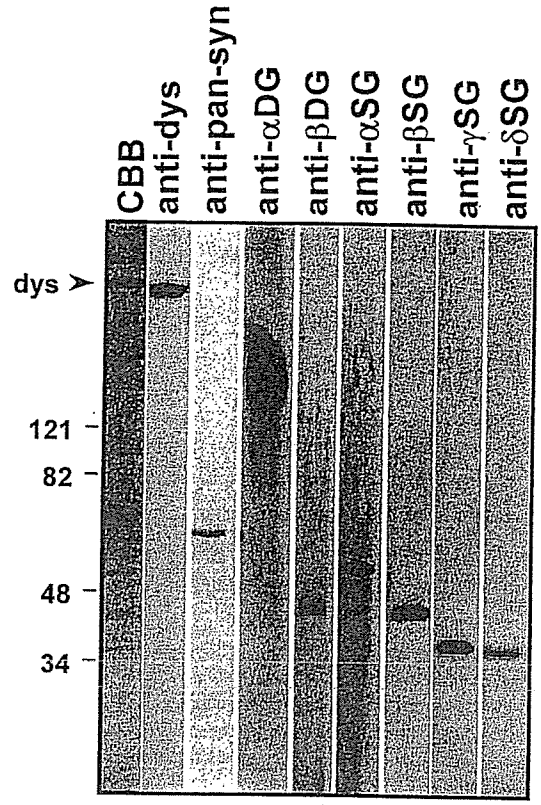

Fig. 1. Components of DGC purified from human cardiac muscle. Digitonin-solubilized human heart were subjected to DEAE-cellulose column and proteins were eluted with the buffer containing 250 mM NaCl and analyzed by SDS-PAGE. Protein bands were visualized by CBB staining (*left*) or by immunoblot with specific antibodies indicated in the figure.

associated proteins with Mr. 62, 60, 57, 52, 45, 43, 35–38 and 24 kDa, as identified by CBB staining on SDS-PAGE (Fig. 1). We attempted further purification of the human cardiac dystrophin-DAP complex by immunoaffinity isolation with anti-dystrophin or anti-α-SG antibody beads and found that the major proteins identified in the DEAE-cellulose-eluate were retained in the eluates from these immunoaffinity beads, suggesting that they are the components of the human cardiac DGC complex (data not shown). We identified these proteins by immunoblot analysis. The 57-kDa protein was recognized by anti-syntrophin antibody SYN1351 that was reported to react with three isoforms of syntrophin [15]. The same result was observed when we used our anti-pan-syntrophin antibody. The broad ~150-kDa protein bands were identified as α-DG by immunoblot with the specific monoclonal antibody M156 (Fig. 1) and by laminin-overlay assay (data not shown), whereas the 45-kD protein was β-DG. The 52-, 43-, 35- and 38-kDa proteins were identified as α-, β- γ -and δ-SGs with specific antibodies against each protein, respectively (Fig. 1). Thus, the purified protein complex from human heart includes all major components of DGC.

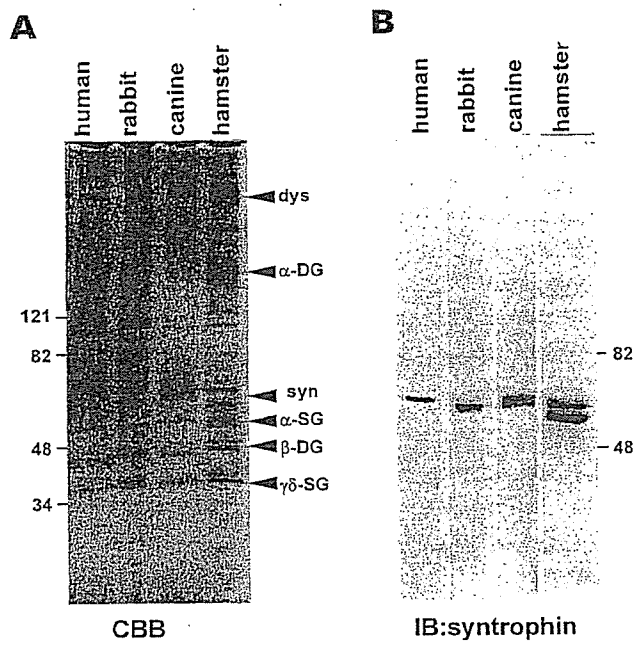

Fig. 2. Comparison of DGC purified from cardiac muscles of different species. DGCs were purified from cardiac muscles of various species and analyzed by SDS-PAGE. Protein bands were visualized by CBB staining (A) or by immunoblot with anti-pan-syntrophin antibody (B).

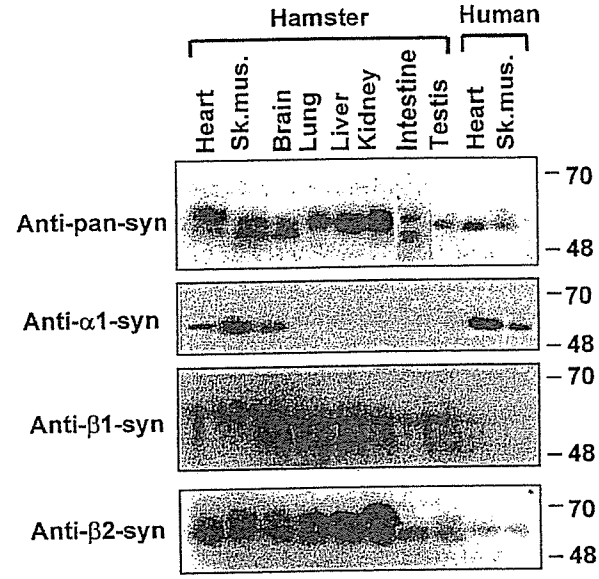

Fig. 3. Expression pattern of syntrophin isoforms in various tissues of hamster and human. Syntrophins were isolated from digitonin-solubilized tissue extracts using anti-pan-syntrophin antibody. The same volume of eluates from beads was subjected to SDS-PAGE and protein bands were visualized by immunoblot with specific antibodies indicated in the figure. Positions of two molecular mass markers (48 and 70 kDa) are shown.

Comparison of cardiac DGC among animal species

We compared the components of DGC from the human cardiac muscle with those from rabbit, canine and hamster cardiac muscles. The DGC from different species contain α- and β-DG, and α-, β-, γ- and δ-SGs with similar apparent molecular masses (Fig. 2A). However, the proteins in the molecular mass range of 57–65 kDa varied among different species (Fig. 2A). We checked whether these protein bands were stained with anti-pan-syntrophin antibody that can recognize all three isoforms of syntrophin. Consistent with a single band detected in CBB-stained gel, only 57 kDa protein was stained with anti-pan-syntrophin antibody in human and rabbit cardiac DGC, while three bands were stained with the same antibody in canine and hamster cardiac DGC.

To distinguish three syntrophin isoforms, we produced isoform-specific antibodies. Syntrophins were first immunoprecipitated with anti-pan-syntrophin antibody and then subjected to immunoblot analysis with each antibody. The α1-, β1- and β2-syntrophins were differently expressed in hamster tissues. The α1-syntrophin was expressed only in heart, skeletal muscle and brain, while β1-syntrophin was expressed in brain, lung, liver and kidney (Fig. 3). On the other hand, β2-syntrophin was expressed ubiquitously in any tissue.

The expression pattern of syntrophin isoforms is consistent with the data performed in mice [19]. However, only α1-syntrophin was detected in human heart and skeletal muscles, consistent again with results for Northern blot analysis previously carried out using RNA from human tissues [1]. We further analyzed species-dependent expression of syntrophin isoforms. Figure 4A shows the immunoblot analysis performed using the purified DGC from hamster or canine cardiac muscles. These DGC samples contained all three syntrophin isoforms with different apparent sizes. We further probed the tissue-homogenates from cardiac or skeletal muscles of various species with anti-pan-syntrophin antibody. Three protein bands were detected in canine, hamster and rat cardiac muscles. In contrast, in cardiac muscles from human, rabbit, bovine and mouse, only a single protein band which corresponds to α-syntrophin was detected (Fig. 4B). On the other hand, three protein bands were detected in skeletal muscles from all species, except human skeletal muscle in which one protein band corresponding to α-syntrophin was detected as a major isoform (Fig. 4B). Of note, apparent molecular masses of syntrophin isoforms are slightly different among species. It is also interesting to note that apparent molecular masses of syntrophins are slightly different between extensor carpi radialis (fast) and superficial digitalis flexor (slow) muscles from the same species (canine). The latter staining pattern is similar to that of canine cardiac muscle.

Subcellular localization of syntrophin isoforms in heart

We examined subcellular localization of syntrophins in cardiac muscles. In hamster cardiac muscle, the α1- and β2-syntrophins were co-localized in sarcolemma and transverse

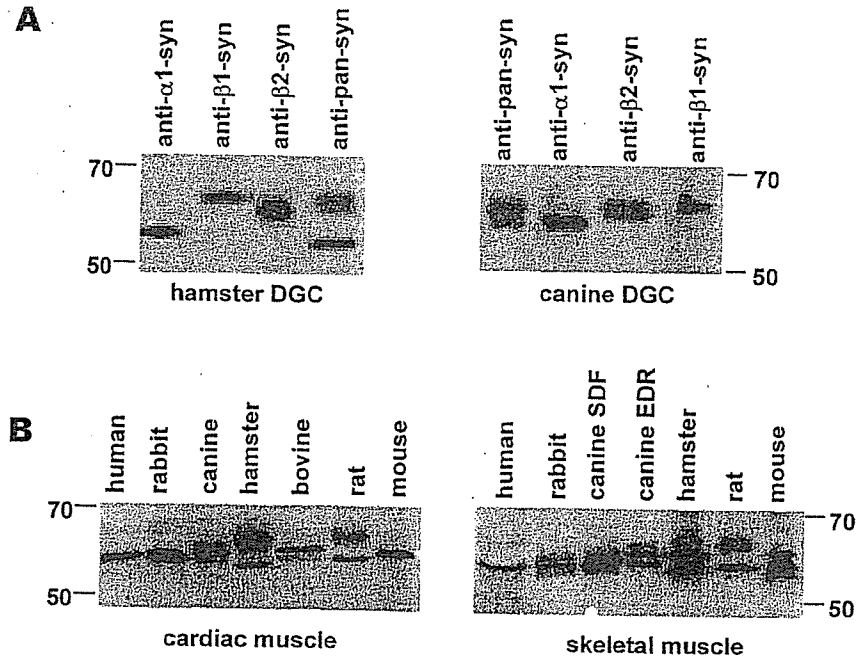

Fig. 4. Expression pattern of syntrophins in different species. (A) DGCs were purified from hamster and canine cardiac muscles and analyzed by immunoblot with anti-pan-syntrophin antibody and isoform-specific antibodies. (B) Cardiac and skeletal muscle homogenates from human, rabbit, canine, hamster, bovine, rat and mouse were subjected to SDS-PAGE and analyzed by immunoblot with anti-pan-syntrophin antibody.

tubule (Fig. 5A). Similar co-localization was observed when muscles were stained with anti β1- (data not shown) or anti-pan-syntrophin antibody (Fig. 5B). These data are in sharp contrast to findings in skeletal muscle in which β2-syntrophins are concentrated in post-synaptic junction, while α1 and β1-syntrophins are expressed entirely in sarcolemma [20]. Of note, in human cardiac muscle α1-syntrophin was localized entirely in sarcolemma (Fig. 5C).

We further carried out subcellular fractionation of human and hamster cardiac muscles. We first homogenized hearts from human and hamster (control and BIO 14.6) in the medium with low ionic strength. After low speed-centrifugation, the supernatant was further separated into cytosolic and membrane fractions by centrifugation (Fig. 6A). Consistent with localization in sarcolemma, considerable amount of syntrophins were recovered together with β-DG in the membrane fraction from hamster and human hearts (Fig. 6B). However, we found that part of syntrophin was also recovered in the cytosol, particularly from cardiac muscle of Bio 14.6 cardiomyopathic hamster (Fig. 6B). We previously reported that much more proteins are extracted from the Bio 14.6 hamster heart as compared to the normal one under homogenization in low ionic strength because of mechanically weak sarcolemma of the cardiomyopathic heart [14]. We thought that the difference in amounts of cytosolic syntrophin between normal and Bio 14.6 hamsters may be due to amounts of proteins extracted under homogenization. Therefore, we homogenized tissues in the presence of high salt (0.5 M NaCl) that improves the efficiency of protein extraction, and found that similar amounts of cytosolic syntrophin were recovered from normal and Bio 14.6 hamster hearts (24 vs. 18% of total syntrophin, respectively), (Fig. 6C).

Discussion

In this study, we purified DGC using hearts from human and other animal species as starting materials. For purification, we homogenized the heart muscle in presence of 1% digitonin. This homogenization much improved the yield of dystrophin extracted from the ventricular muscle. This method would be particularly important when only a limited amount of tissues are available. This improved method would be useful to purify DGC from biopsy sample from human patients with cardiac disease to obtain the information on DGC in heart failure. We observed that almost all components of DGC were present in the purified complex proteins from hearts in human and other animal species, although the amount of dystrophin in human DGC was lower than that in other animals (Fig. 2). Interestingly, the pattern of syntrophin isoforms with apparent molecular masses of 50–65 kDa was different among species. All three isoforms of syntrophin (α1, β1, β2) were expressed in hamster, rat and canine ventricles, while only α1; isoform was mainly expressed in human and rabbit ventricles (Fig. 4). Thus, in cardiac muscle there are species-dependent variations in expression pattern of syntrophin isoforms. Some of

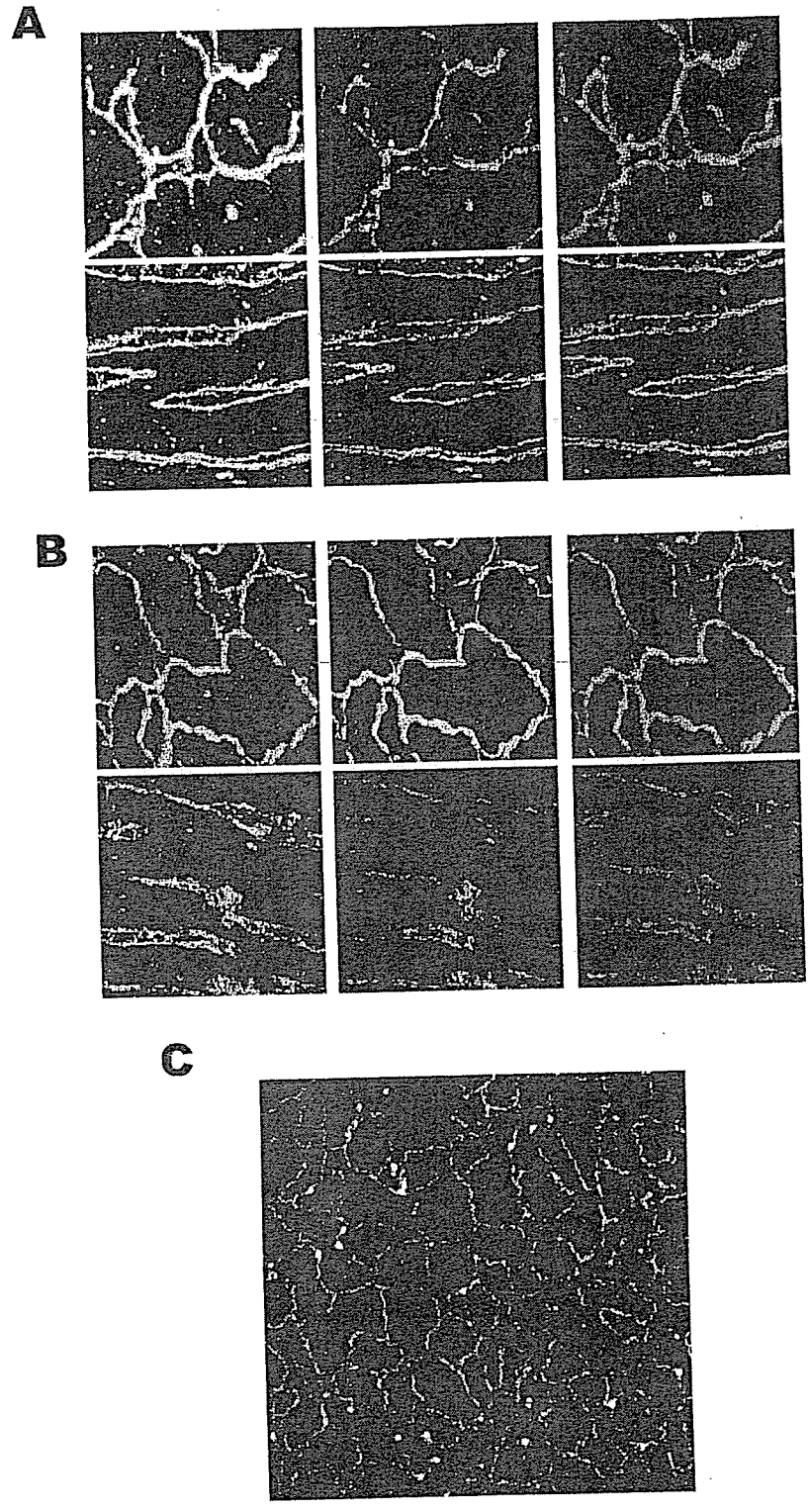

Fig. 5. Subcellular localization of syntrophins in canine ventricular muscles. (A) Cross (*upper panel*) and longitudinal sections (*lower panel*) of canine ventricular muscles were stained with anti- α1-(*left*) and anti-β2-syntrophins (*middle*). (B) Sections of canine ventricular muscles were stained with anti-β1-(*left*) and anti-pan-syntrophin antibodies (*middle*). Antibody specificity was confirmed in adjacent serial sections by preincubating antibodies with the appropriate antigenic peptide or antigenic fusion protein (not shown). Merged photographs are shown in the right panels and overlapping regions stained with anti-α1/anti-β2 or anti-α1/anti-pan syntrophin antibodies are represented by yellow color. Original color information (*red* and *green*) was omitted in the figures (*left* and *middle*). (C) Cross section of human cardiac muscle was stained with anti-pan-syntrophin antibody.

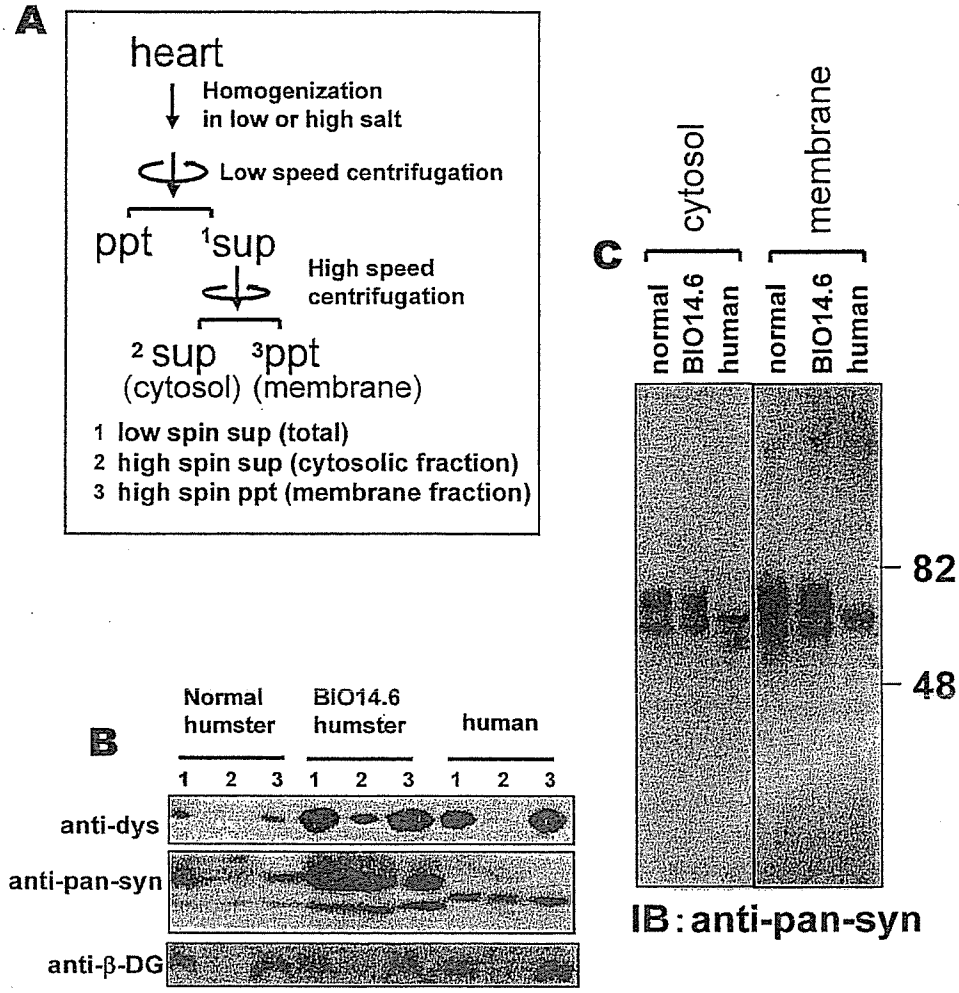

Fig. 6. Subcellular fractionation of cardiac muscles. Syntrophins exist both in cytosolic and membrane fraction. (A) Schematic drawing of subcellular fractionation. Ventricular muscles (0.1 g) from normal and BIO14.6 hamsters, and human biopsy sample were fractionated as described under "Materials and Methods". Proteins were analyzed by immunoblot with anti-dystrophin, anti-pan-syntrophin and anti-β-dystroglycan antibodies respectively (A) (1; total, 2; cytosolic fraction, 3, membrane fraction). (C) Tissues were homogenized with high salt (0.5 M NaCl), and fractionated into the cytosol and membrane fractions. The latter was solubilized with detergent (1% NP40 0.1% SDS, 0.1%DOC). The cytosol and detergent-solubilized membrane fractions were incubated with anti-α-syntrophin antibody conjugated-immunoaffmity beads. Proteins eluted from beads were analyzed by immunoblot with anti-pan-syntrophin antibody.

these findings are consistent with previous reports [1, 19] in which expression of syntrophin isoforms was checked by only Northern blot analysis.

Immunohistochemical analysis revealed that α1- and β2-syntrophins were co-localized in sarcolemma and in T-tubules of canine ventricles, in contrast to a report that β2-syntrophin was localized in neuromuscular junction together with utrophin in skeletal muscle [20]. Localization of β2-syntrophin in neuromuscular junction was also confirmed in canine skeletal muscle by immunohistochemistry (our unpublished observation). Despite membrane localization of most syntrophins, subcellular fractionation revealed that in addition to membrane fraction, part of cardiac syntrophins were also recovered in the cytosolic fraction where other components of DGC were not detected (Fig. 6). We observed that the complex of syntrophin with dystrophin was not disrupted by treatment with 1% digitonin, suggesting strong interaction between these proteins (Iwata *et al.*, unpublished observation). Therefore, it is unlikely that syntrophins are easily removed from membranes under extraction with low ionic strength. Rather, it is likely that some syntrophins do not interact with DGC in cells. In fact, syntrophins were reported to bind to various proteins, such as F-actin [21], Calmodulin [21, 22], phosphatidylinositol bisphosphate [23], dystrobrevin [24], nNOS [25] and Na channel [26]. Some syntrophins recovered in the cytosolic fraction (Fig. 6) may be derived from these interacting proteins. However, we could not detect the syntrophin localization in the cytosol or in some intracellular compartments of cardiac muscle. We do not exclude the possibility that

cytosolic syntrophins may be removed during the tissue fixation and permeabilization.

In summary, we found that the expression pattern of syntrophin isoforms greatly depends on the muscle-type and species. In addition, our data suggested that part of syntrophins exists as a form(s) not associated with DGC in cardiac muscle. These properties may provide an important clue to explain why the severity of muscle dysgenesis caused by the primary defect in components of DGC is sometimes different between skeletal and cardiac muscles or between human patients and other animal species.

Acknowledgments

We thank Dr. Chikao Yutani at the Department of Pathology in National Cardiovascular Center for the generous provision of human specimens. This work was supported by Grant-in-Aid for Priority Areas 13142210 and Grant-in-Aid 14580664 and 14570708 from the Ministry of Education, Culture, Sports, Science and Technology of Japan and by a grant for Promotion of Fundamental Studies in Health Science from the Organization of Pharmaceutical Safety and Research.

References

1. Hunsaker RH, Fulkerson PK, Barry FJ, Lewis RP, Leier CV, Unverferth DV: Cardiac function in Duchenne's muscular dystrophy Results of 10-year follow-up study and noninvasive tests. Am J Med 73: 235–238, 1982
2. Torres LF, Duchen LW: The mutant *mdx*: Inherited myopathy in the mouse. Morphological studies of nerves, muscles and end-plates. Brain 110: 269–299, 1987
3. Towbin JA, Hejtmancik JF, Brink P, Gelb B, Zhu XM, Chamberlain JS, McCabe ERB, Swift M: X-linked dilated cardiomyopathy molecular genetic evidence of linkage to the Duchenne muscular dystrophy (dystrophin) gene at the Xp21 locus. Circulation 87: 1854–1865, 1993
4. Piccolo F, Roberds SL, Jeanpierre M, Leturcq F, Azibi K, Beldjord C, Carrié A, Récan D, Chaouch M, Reghis A, El Kerch F, Sefiani A, Voit T, Merlini L, Collin H, Eymard B, Beckmann JS, Romero NB, Tomé FMS, Fardeau M, Campbell KP, Kaplan J-C: Primary adhalinopathy: A common cause of autosomal recessive muscular dystrophy of variable severity. Nature Genetics 10: 243–245, 1995
5. Roberds SL, Ervasti JM, Anderson RD, Ohlendieck K, Kahl SD, Zoloto D, Campbell KP: Disruption of the dystrophin-glycoprotein complex in the cardiomyopathic hamster. J Biol Chem 268: 11496–11499, 1993
6. Ahn AH, Kunkel LM: The structural and functional diversity of dystrophin. Nature Genetics 3: 283–291, 1993
7. Klietsch R, Ervasti JM, Arnold W, Campbell KP, Jorgensen AO: Dystrophin-glycoprotein complex and laminin colocalize to the sarcolemma and transverse tubules of cardiac muscle. Circ Res 72: 349–360, 1993
8. Frank JS, Mottino G, Chen F, Peri V, Holland P, Tuana BS: Subcellular distribution of dystrophin in isolated adult and neonatal cardiac myocytes. Am J Physiol 267: C1707–C1716, 1994
9. Meng H, Leddy JJ, Frank J, Holland P, Tuana BS: The association of cardiac dystrophin with myofibrils/Z-disc regions in cardiac muscle suggests a novel role in the contractile apparatus. J Biol Chem 271:12364–12371, 1996
10. Rivier F, Robert A, Hugon G, Bonet-Kerrache A, Nigro V, Fehrentz JA, Martinez J, Mornet D: Dystrophin and utrophin complexed with different associated proteins in cardiac Purkinje fibers. Histochem J 31: 425–432, 1999
11. Ahn AH, Freener CA, Gussoni E, Yoshida M, Ozawa E, Kunkel LM: The three human syntrophin genes are expressed in diverse tissues have distinct chromosomal locations and each bind to dystrophin and its relatives. J Biol Chem 271: 2724–2730, 1996
12. Piluso G, Mirabella M, Ricci E, Belsito A, Abbondanza C, Servidei S, Puca AA, Tonali P, Puca GA, Nigro V: γ1- and γ2-Syntrophins, two novel dystrophin-binding proteins localized in neuronal cells. J Biol Chem 275: 15851–15860, 2000
13. Iwata Y, Pan Y, Hanada H, Yoshida T, Shigekawa M: Dystrophin-dystrophin associated protein complex purified from hamster cardiac muscle. Comparison of the complexes from cardiac and skeletal muscles of hamster and rabbit. J Mol Cell Cardiol 28: 2501–2509, 1996
14. Tawada-Iwata Y, Imagawa T, Yoshida A, Takahashi M, Nakamura H, Shigekawa M: Increased mechanical extraction of T-tubule/junctional SR from cardiomyopathic hamster heart. Am J Physiol 264: H1447–H1453, 1993
15. Matthew P, Adams ME, Froehner SC: Differential association of syntrophin pairs with the dystrophin complex. J Cell Biol 138: 81–93, 1997
16. Sampaolesi M, Yoshida Y, Iwata Y, Hanada H, Shigekawa M: Stretch-induced cell damage in sarcoglycan-deficient myotubes. Pflugers Arch 442: 161–170, 2001
17. Froehner SC, Murnane AA, Tobler M, Peng HB, Sealock R: A post-synaptic Mr 58000 (58k) protein concentrate at acetylcholine receptor-rich sites in Torpedo electroplaques and skeletal muscle. J Cell Biol 104: 1633–1646, 1987
18. Iwata Y, Nakamura H, Mizuno Y, Yoshida M, Ozawa E, Shigekawa, M: Defective association of dystrophin with sarcolemmal glycoproteins in the cardiomyopathic hamster heart. FEBS Lett 329: 227–231, 1993
19. Peters MF, Adams ME, Froehner SC: Differential association of syntrophin pairs with the dystrophin complex. J Cell Biol 138: 81–93, 1997
20. Matthew FP, Kramarcy NR, Sealock R, Froehner SC: β2-Syntrophin: Localization at the neuromuscular junction in skeletal muscle. Neuro Report 5: 1577–1580, 1994
21. Iwata Y, Pan Y, Yoshida T, Hanada H, Shigekawa M: α1-Syntrophin has distinct binding sites for actin and calmodulin. FEBS Lett 423: 173–177, 1998
22. Newbell BJ, Anderson JT, Jarrett HW: Ca^{2+}-calmodulin binding to mouse alphal syntrophin: Syntrophin is also a Ca^{2+}-binding protein. Biochemistry 36: 1295–305, 1997
23. Chockalingam PS, Gee SH, Jarrett HW: Pleckstrin homology domain 1 of mouse α1-syntrophin binds phosphatidylinositol 4,5-biphosphate. Biochemistry 38: 5596–5602, 1999
24. Dwyer TM, Froehner SC: Direct binding of Torpedo syntrophin to dystrophin and the 87 kDa dystrophin homologue. FEES Lett 375: 91–94, 1995
25. Brenman JE, Chao DS, Gee SH, McGee AW, Craven SE, Santillano DR, Wu Z: Interaction of nitric oxide synthase with the postsynaptic density protein PSD-95 and alphal-syntrophin mediated by PDZ domains. Cell 84: 757–767, 1996
26. Gee SH, Madhavan R, Levinson SR, Caldwell JH, Sealock R, Froehner SC: Interaction of muscle and brain sodium channels with multiple members of the syntrophin family of dystrophin-associated proteins. J Neurosci 274: 128–137, 1998

MCBI-5382998

THE JOURNAL OF BIOLOGICAL CHEMISTRY
Vol. 280, No. 7, Issue of February 18, pp. 5764–5772, 2005
Printed in U.S.A.
© 2005 by The American Society for Biochemistry and Molecular Biology, Inc.

Calcineurin Inhibits Na^+/Ca^{2+} Exchange in Phenylephrine-treated Hypertrophic Cardiomyocytes*

Received for publication, September 7, 2004, and in revised form, November 4, 2004
Published, JBC Papers in Press, November 22, 2004, DOI 10.1074/jbc.M410240200

Yuki Katanosaka‡§, Yuko Iwata‡, Yuko Kobayashi‡, Futoshi Shibasaki¶, Shigeo Wakabayashi‡, and Munekazu Shigekawa‡‖**

From the ‡Department of Molecular Physiology, National Cardiovascular Center Research Institute, Fujishiro-dai 5-7, Suita, Osaka 565-8565, the ¶Department of Molecular Cell Physiology, The Tokyo Metropolitan Institute of Medical Science, Honkomagome 3-18-22, Bunkyo-ku, Tokyo 113-8613, and the ‖Department of Human Life Sciences, Senri-Kinran University, Fujishiro-dai 5-25-1, Suita, Osaka 565-0873 Japan

The cardiac Na^+/Ca^{2+} exchanger (NCX1) is the predominant mechanism for the extrusion of Ca^{2+} from beating cardiomyocytes. The role of protein phosphorylation in the regulation of NCX1 function in normal and diseased hearts remains unclear. In our search for proteins that interact with NCX1 using a yeast two-hybrid screen, we found that the C terminus of calcineurin Aβ, containing the autoinhibitory domain, binds to the β1 repeat of the central cytoplasmic loop of NCX1 that presumably constitutes part of the allosteric Ca^{2+} regulatory site. The association of NCX1 with calcineurin was significantly increased in the BIO14.6 cardiomyopathic hamster heart compared with that in the normal control. In hypertrophic neonatal rat cardiomyocytes subjected to chronic phenylephrine treatment, we observed a marked depression of NCX activity measured as the rate of Na^+_i-dependent $^{45}Ca^{2+}$ uptake or the rate of Na^+_o-dependent $^{45}Ca^{2+}$ efflux. Depressed NCX activity was partially and independently reversed by the acute inhibition of calcineurin and protein kinase C activities with little effect on myocyte hypertrophic phenotypes. Studies of NCX1 deletion mutants expressed in CCL39 cells were consistent with the view that the β1 repeat is required for the action of endogenous calcineurin and that the large cytoplasmic loop may be required to maintain the interaction of the enzyme with its substrate. Our data suggest that NCX1 is a novel regulatory target for calcineurin and that depressed NCX activity might contribute to the etiology of *in vivo* cardiac hypertrophy and dysfunction occurring under conditions in which both calcineurin and protein kinase C are chronically activated.

The Na^+/Ca^{2+} exchanger (NCX)[1] catalyzes the reversible exchange of Na^+ for Ca^{2+} across the plasma membrane. In normal cardiac muscle, the primary role of NCX1 (the cardiac isoform of NCX) is to extrude cytoplasmic Ca^{2+} during myocyte repolarization and diastole, which balances Ca^{2+} entry via L-type Ca^{2+} channels during myocyte depolarization (1, 2). The transport activity of NCX1 is known to be influenced by a variety of factors, including hormones and growth factors, intracellular Na^+ and Ca^{2+} concentrations, membrane potential, cytoplasmic ATP, and protein and lipid phosphorylation (3). However, information is still limited as to the quantitative aspects of changes in these factors and their consequences on NCX1 activity in normal and diseased cardiomyocytes. For example, in hypertrophic and failing hearts from human patients and animal models, sarcolemmal NCX1 expression has often been shown to be elevated (4–7), which could be compensatory for the reduced ability of the sarcoplasmic reticulum to maintain low diastolic $[Ca^{2+}]_i$ under these pathological conditions. However, whether increased NCX expression invariably leads to enhanced function under disease conditions is not clear, although enhanced NCX expression and function have been observed in cardiomyocytes isolated from some animal models of cardiac hypertrophy and heart failure (6, 7).

Protein phosphorylation is an important mechanism regulating the functions of many cellular systems. In the case of NCX1, acute treatment with PMA or agonists of $G\alpha_q$-coupled receptors such as phenylephrine (PE) has been shown to enhance NCX activity in isolated cardiomyocytes as well as in cells expressing cloned NCX1 (8–10). Protein kinase A activation has also been reported to stimulate NCX1 activity (11, 12). On the other hand, a protein phosphatase inhibitor, calyculin A, reportedly causes substantial inhibition of NCX activity in cells expressing cloned NCX1 (13). NCX1 stimulation by PMA and agonists of $G\alpha_q$-coupled receptors occurs via a mechanism involving PKC activation and requires the participation of the central cytoplasmic loop of the exchanger (see Fig. 1*a*) (9). Because these agonist effects did not require the direct phosphorylation of NCX1, the central cytoplasmic loop was considered to serve as an anchor for phosphorylatable regulatory ancillary protein(s) (9).

In this study, we undertook a search for regulatory proteins interacting with the central cytoplasmic loop of NCX1 by using a yeast two-hybrid screen. From this search and subsequent analysis, we identified a complex, hitherto unrecognized regulatory mechanism for cardiac NCX1 involving calcineurin and PKC in hypertrophic cardiomyocytes subjected to prolonged PE pretreatment. This mechanism is capable of markedly depressing NCX1 activity. Because calcineurin acts as a central medi-

* This work was supported by Special Coordination Funds from the Ministry of Education, Culture, Sports, Science and Technology, a Grant for Promotion of Fundamental Studies in Heath Science from the Organization of Pharmaceutical Safety and Research, and a grant from the Uehara Foundation. The costs of publication of this article were defrayed in part by the payment of page charges. This article must therefore be hereby marked "*advertisement*" in accordance with 18 U.S.C. Section 1734 solely to indicate this fact.

§ Research Fellow of the Japan Society for the Promotion of Science.
** To whom correspondence should be addressed. Tel.: 81-6-6872-7846; Fax: 81-6-6872-7872; E-mail: shigekaw@ri.ncvc.go.jp.

[1] The abbreviations used are: NCX, Na^+/Ca^{2+} exchanger; NCX1, cardiac isoform of NCX; aa, amino acids; ANP, atrial natriuretic peptide; BSS, balanced salt solution; CnA, calcineurin A; DOX, doxycycline; FCS, fetal calf serum; PE, phenylephrine; PKC, protein kinase C; PMA, phorbol 12-myristate 13-acetate; Rp-8-CPT-cAMPS, 8-(4-chlorophenylthio)adenosine-3′,5′-cyclic monophosphorothioate; Rp-8-CPT-cGMPS, 8-(4-chlorophenylthio)guanosine-3′,5′-cyclic monophosphorothioate; TUNEL, terminal deoxynucleotidyltransferase-mediated dUTP nick end-labeling.

This paper is available on line at http://www.jbc.org

ator of *in vivo* cardiac hypertrophy and failure (14–16), NCX might contribute to the etiology of *in vivo* cardiac dysfunction.

EXPERIMENTAL PROCEDURES

Materials—FCS, PE, FK506, PMA, calphostin C, 8-bromo-cAMP, Rp-8-CPT-cAMPS, 8-bromo-cGMP, Rp-8-CPT-cGMPS, and H89 were purchased from Sigma. GF109203X, chelerythrine chloride, KN93, and KN62 were purchased from Calbiochem. Rhodamine-conjugated phalloidin was obtained from Molecular Probes. Antibodies to NCX isoforms have been described (8, 9). Rabbit polyclonal anti-pan calcineurin A (CnA) and goat polyclonal anti-CnAβ (Santa Cruz Biotechnology), mouse monoclonal anti-CnAβ (Upstate Technology), anti-hemagglutinin (Roche Applied Science), rabbit polyclonal anti-atrial natriuretic peptide (anti-ANP; Phoenix Pharmaceuticals), fluorescein isothiocyanate-conjugated anti-rabbit IgG and rhodamine-conjugated anti-goat IgG (ICN/CAPEL), and anti-calmodulin, horseradish peroxidase-conjugated anti-rabbit IgG, and biotin-conjugated anti-mouse IgG (Zymed Laboratories Inc.) were purchased the from the sources indicated in parentheses. Horseradish peroxidase-conjugated streptavidin was obtained from Zymed Laboratories Inc.. $^{45}CaCl_2$ was purchased from Amersham Biosciences.

Animals—Pregnant Wister rats and male Bio14.6 hamsters (J2N-k strain, 120 days old) and age-matched normal controls (J2N-n) were purchased from Japan SLC. The J2N-n had the same genetic background as the J2N-k, except for the difference of a genetic locus for cardiomyopathy.

Cell Cultures—Primary cardiomyocyte cultures were prepared from ventricles of 1-day-old rats as described previously (17). They were plated on collagen-coated 24-well dishes at a density of 4×10^6 cells per well and maintained in M199 medium supplemented with 10% FCS. Staining with rhodamine-phalloidin revealed that >90% of the cells were cardiomyocytes. Two days later, the cells were divided into three groups and then maintained for up to 5 days in M199 alone, M199 with 10 μM PE, or M199 with 10% FCS (see Fig. 3*a*). These myocytes usually form clusters and exhibit spontaneous synchronized beating (17). On the other hand, CCL39 cells (American Type Culture Collection) and their NCX1 transfectants were maintained in Dulbecco's modified Eagle's medium containing 7.5% FCS, 50 units/ml penicillin, and 50 μg/ml streptomycin.

Construction of Vectors and Expression of NCX1 and Calcineurin—The preparation of cDNAs of dog heart NCX1 and NCX1 mutants lacking aa 246–672 (NCX1Δ246–672) or aa 407–478 (NCX1Δ407–478), their transfection into CCL39 cells, and the isolation of cell clones stably expressing high NCX activity were carried out as described previously (8, 9). The isolation of cDNA encoding human CnAβ and the construction of its constitutively active mutant (ΔCnA) lacking the autoinhibitory and the calmodulin binding domains were described previously (18, 19). A catalytically inactive mutant of CnA that functions as a dominant negative mutant was prepared from ΔCnA by mutating histidine at position 160 to glutamine (19). Hemagglutinin-tagged wild-type and mutant CnAβs were subcloned into an adenoviral vector downstream of the Tet-Off system (18). Cardiomyocytes were infected with adenoviral vectors at a multiplicity of infection of 100 plaque-forming units per cell in serum-free M199 medium for 2 h at 37 °C. Efficiency of infection under these conditions was 100%, as revealed by immunostaining with an anti-hemagglutinin antibody. In control cells, the expression of adenoviral vectors was suppressed with 1 μM doxycycline (DOX) added to culture medium.

Yeast Two-hybrid Screen—We used Matchmaker 3 (Clontech) for the yeast two-hybrid screen. DNA fragments corresponding to the following segments of the central cytoplasmic loop of dog NCX1, shown in Fig. 1*a*, were prepared using a PCR-based method: the NCX inhibitory peptide (*XIP*, Fig. 1*a*), aa 250–406; β1, aa 407–478; β1-β2, aa 479–538; β2, aa 539–613; C terminus (*CT*, Fig. 1*a*), aa 614–796; N terminus (*NT*, Fig. 1*a*), aa 250–613; and the full loop (*Full*, Fig. 1*a*), aa 250–796. Each DNA fragment was fused to the GAL4 DNA binding domain in the pGBKT7 vector. We used a mixture of yeasts carrying each of these bait constructs for the initial screening of ~4×10^7 clones from a human brain cDNA library fused to the GAL4 activation domain. These bait and library yeast strains were mated by culturing on agar plates in complete YPD (1% yeast extract, 2% peptone, and 2% glucose) medium overnight at 20 °C. After successive screening in medium lacking histidine, leucine, and tryptophan (−*HLT*, Fig. 1*b*) and then in medium lacking histidine, adenine, leucine, and tryptophan (−*HALT*, Fig. 1*b*), grown-up colonies were isolated and subjected to β-galactosidase assay according to the manufacturer's instructions. The inserts in β-galactosidase-positive clones were sequenced using the activation domain sequence primers by the ABI 9600 sequencer. Positive clones were verified by one-on-one transformations and selections by growth on agar plates in −HALT medium and β-galactosidase assay (see Fig. 1*b*).

Immunoprecipitation, Immunoblot, and Immunocytochemical Analyses—Brain and/or ventricular tissues from rat or hamster and cultured rat cardiomyocytes were homogenized by Hiscotron (NITI-ON, Funabashi, Japan) in radioimmune precipitation assay lysis buffer containing 20 mM HEPES (pH 7.4), 150 mM NaCl, 1% sodium deoxycholate, 1% Triton X-100, 0.1% SDS, 2 μg/ml leupeptin, 1 μg/ml aprotinin, 200 μM phenylmethylsulfonyl fluoride, and 200 μM benzamidine hydrochloride. The lysates were subjected to centrifugation at 100,000 × *g* for 20 min, and the resultant supernatant (up to 5 mg protein) was pre-cleared with 50 μl of protein A-Sepharose beads for 2 h at 4 °C on a rotator. After centrifugation, the supernatant was incubated with anti-pan CnA for 2 h at 4 °C and then with 50 μl of protein A-Sepharose beads for at least 2 h at 4 °C on a rotator. The beads were washed eight times with ice-cold phosphate-buffered saline. Proteins solubilized from beads by boiling in the Laemmli buffer (20) were subjected to SDS-PAGE on a 8.5% gel and then to immunoblotting with an appropriate antibody. Immunoblot analysis was performed essentially as described previously (21). The immunoblot was visualized using an enhanced chemiluminescence detection system (Amersham Biosciences).

For immunocytochemistry, 5-μm-thick sections of normal and BIO14.6 hamster ventricular tissues embedded in OCT compound (Tissue-Tek) were permeabilized with 0.1% Triton X-100 and treated with rabbit polyclonal anti-NCX1 or goat polyclonal anti-CnAβ at dilutions of 1:500 and 1:200, respectively. These samples were then treated with fluorescein isothiocyanate-conjugated anti-rabbit IgG or rhodamine-conjugated anti-goat IgG. For immunostaining of rat cardiomyocytes, cells immobilized on collagen-coated glass slides were fixed with 4% paraformaldehyde for 15 min at room temperature, permeabilized with 0.1% Triton X-100, and then stained with anti-NCX1, anti-pan CnA, or anti-ANP. For double staining with a combination of polyclonal (rabbit) and monoclonal (mouse) antibodies, fixed and permeabilized myocytes were incubated with a mixture of two primary antibodies and then with a mixture of the fluorescence-labeled anti-mouse and rhodamine-labeled anti-rabbits IgGs. Cells were examined by a confocal laser scanning microscopy (MRC-1024, Bio-Rad) mounted on an Olympus BX50WI epifluorescence microscope with a plan-apochromat 60× water immersion objective lens (Olympus).

Fractionation of Heart Extracts—Normal and BIO14.6 hamster hearts were homogenized in phosphate-buffered saline using a Hiscotron homogenizer and centrifuged at 15,000 × *g* for 15 min. The resultant supernatant was centrifuged at 500,000 × *g* for 45 min to yield supernatant and pellet fractions. Most of the sarcolemmal and sarcoplasmic reticulum membranes were presumably recovered in the pellet fraction. Both the supernatant and pellet fractions were then subjected to immunoblot analysis with anti-pan CnA.

Na^+_i-dependent $^{45}Ca^{2+}$ Uptake into and Na^+_o-dependent $^{45}Ca^{2+}$ Efflux from Cells—Na^+_i-dependent $^{45}Ca^{2+}$ uptake into cells was measured as described previously (8, 9, 22) with slight modifications. Cardiomyocytes or CCL39 cells cultured in 24-well dishes were loaded with Na^+ by incubating them at 37 °C for 30 min in 0.5 ml of normal BSS (10 mM Hepes/Tris (pH7.4), 146 mM NaCl, 4 mM KCl, 2 mM $MgCl_2$, 0.1 mM $CaCl_2$, 10 mM glucose, and 0.1% bovine serum albumin) containing 1 mM ouabain and 10 μM monensin. In cardiomyocytes pretreated with PE or FCS, Na^+ loading was carried out during the last 30 min of such pretreatment. $^{45}Ca^{2+}$ uptake was then initiated by switching the medium to Na^+-free BSS containing choline chloride or to normal BSS, both of which contained 370 kBq of $^{45}Ca^{2+}$ and 1 mM ouabain. After a 30-s incubation, cells were washed with an ice-cold solution containing 10 mM $LaCl_3$ to stop $^{45}Ca^{2+}$ uptake. Cells were subsequently solubilized with 0.1 N NaOH, and aliquots were taken for the determination of radioactivity and protein. Na^+_i-dependent $^{45}Ca^{2+}$ uptake was estimated by subtracting $^{45}Ca^{2+}$ uptake in normal BSS from that in Na^+-free BSS. To observe the effects of FK506, protein kinase modulators, or thapsigargin, cells were incubated with these substances during the last 15–30 min of Na^+ loading, except that endogenous PKC was down-regulated by treatment with 0.3 μM PMA for 24 h. The Na^+_i-dependent $^{45}Ca^{2+}$ uptake activities in control cells not pretreated with PE or other agents were as follows: for cardiomyocytes, 12.1 ± 0.5 nmol/mg/30s (n = 9); for CCL39 cells expressing the wild-type NCX1, NCX1Δ246–672, and NCX1Δ407–478, 10.4 ± 0.5, 4.2 ± 0.4, and 5.3 ± 0.2 nmol/mg/30s (n = 9), respectively. These values were taken as 100% in Figs. 3*d*, 4*a*, 5, 6, and 7.

To measure $^{45}Ca^{2+}$ efflux, cardiomyocytes in 35-mm dishes were incubated in 1 ml BSS containing 740 kBq of $^{45}Ca^{2+}$ for the last 2 and

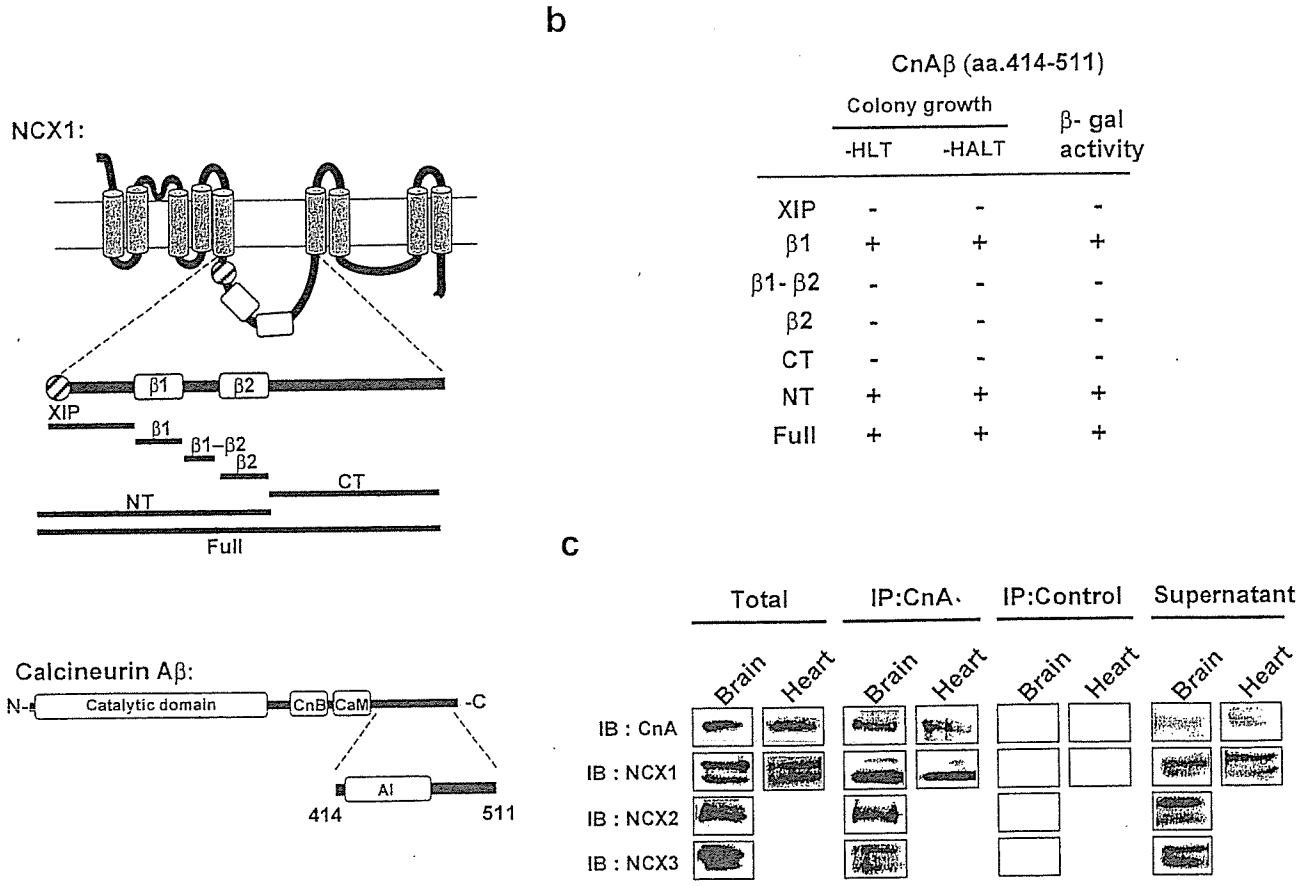

FIG. 1. **Identification of CnAβ as a NCX-binding protein.** *a*, domain structures of NCX1 and CnAβ. Segments of the central cytoplasmic loop of NCX1, labeled as indicated (*XIP*, NCX inhibitory peptide; *NT*, N terminus; *CT*, C terminus), were used as bait for the yeast two-hybrid screen. In CnAβ, *CnB*, *CaM*, and *AI* are the calcineurin B binding, the calmodulin binding, and the autoinhibitory domains, respectively. *b*, colony growth after one-on-one transformation and selection in medium lacking histidine, leucine, and tryptophan (*−HLT*) or medium lacking histidine, alanine, leucine, and tryptophan (*−HALT*) and β-galactosidase (*β-gal*)-positive colonies in −HALT medium. *c*, co-immunoprecipitation of CnA with NCX isoforms. Lysates from rat brain and heart (*Total*), materials immunoprecipitated with anti-pan CnA (*IP:CnA*) or no antibody (*IP:control*), and post-immunoprecipitation supernatants (*Supernatant*) were subjected to immunoblot (*IB*) assays with antibodies to the indicated proteins.

4 h of the 72-h treatment with and without 10 μM PE, respectively, which produced essentially the same level of $^{45}Ca^{2+}$ loading in PE-treated and non-treated cells. After rinsing cells six times with Ca^{2+}- and Na^+-free BSS for 1 min, $^{45}Ca^{2+}$ efflux was measured for 20 s in Ca^{2+}- and Na^+-free BSS or in Ca^{2+}-free BSS, both of which contained 1 μM thapsigargin, to acutely increase $[Ca^{2+}]_i$ (23). Na^+_o-dependent $^{45}Ca^{2+}$ efflux was estimated by subtracting $^{45}Ca^{2+}$ efflux in Ca^{2+}- and Na^+-free BSS from that in Ca^{2+}-free BSS.

Detection of TUNEL-positive Cells—For *in situ* detection of DNA fragmentation, we assayed TUNEL-positive cells using an apoptosis detection kit (Takara Biomedical) essentially as described previously (24). The number of TUNEL-labeled nuclei was counted by observing rat cardiomyocytes with a light microscope (40× objective; Olympus). TUNEL-positive cells were <3% in normal cardiomyocytes.

Data Analysis—Reproducibility of the data presented in the figures and those described in the text was confirmed in at least three independent experiments. Significant differences between two groups of data were evaluated by an analysis of variance assay with *post hoc* tests. $p < 0.05$ was considered as a statistically significant finding.

RESULTS

Isolation of CnAβ as a NCX1-binding Protein and Mapping of the Interacting Site in NCX1—To isolate protein(s) interacting with NCX1, we performed the yeast two-hybrid screen of a human brain cDNA library using various segments of the large central loop of NCX1 as bait (Fig. 1*a*). From an initial screen in which we used a mixture of yeast populations expressing individual bait sequences, we isolated a positive clone encoding a ~100 amino acid C-terminal tail of CnAβ with its autoinhibitory domain (Fig. 1*a*). We then examined the interaction of individual NCX segments with the CnAβ tail by one-on-one transformations and selection by colony growth and β-galactosidase assays (Fig. 1*b*). We confirmed that aa 407–478 of the NCX1 protein, known as the β1 repeat, and other fragments containing this same sequence associate with the CnAβ tail.

We examined whether calcineurin interacts with NCX1 and its isoforms (NCX2 and NCX3) at the protein level. We found that anti-pan CnA co-precipitated proteins reactive with antibody to each isoform from lysates of rat brain and heart, although these proteins were still relatively abundant in the supernatant fractions (Fig. 1*c*). Thus, at least some calcineurin was physically associated with NCX isoforms, consistent with the fact that the β1 repeat sequence is conserved in these isoforms. Of note, anti-pan CnA immunoprecipitated single major proteins from rat (Fig. 1*c*) and hamster (Fig. 2*b*) hearts that were recognized by anti-CnAβ, indicating that the antibody predominantly precipitated CnAβ under the conditions used.

Enhanced Association of CnAβ with NCX1 in BIO14.6 Hamster Heart—The BIO14.6 hamsters develop cardiomyopathy and muscular dystrophy due to δ-sarcoglycan deficiency (25, 26). We examined the interaction of NCX1 with calcineurin in the hearts of 120-day-old BIO14.6 hamsters, because our recent study has suggested that $[Ca^{2+}]_i$ might be elevated in BIO14.6 cardiomyocytes due to increased basal Ca^{2+} influx (27). Anti-CnAβ immunoprecipitated more abundant NCX1

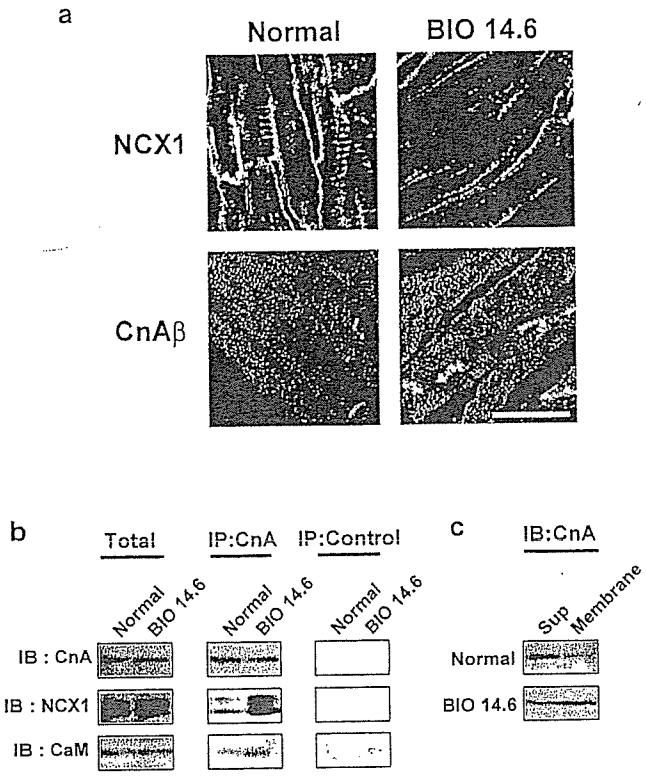

FIG. 2. **Subcellular localization of NCX1 and CnAβ in normal and BIO14.6 hamster hearts.** *a*, immunostaining of hamster ventricular muscle with anti-NCX1 or anti-CnAβ. *Bar*, 20 μm. *b*, co-immunoprecipitation of NCX1 and calmodulin (*CaM*) with CnA. Lysates of normal and BIO14.6 hamster ventricular muscles (*Total*) and materials immunoprecipitated with anti-pan CnA (*IP:CnA*) or no antibody (*IP: control*) were subjected to immunoblot analyses with antibodies to the indicated proteins. *c*, subcellular fractionation of normal and BIO14.6 hamster ventricular homogenates followed by immunoblot (*IB*) assays of membrane and supernatant (*Sup*) fractions with anti-pan CnA.

protein from BIO14.6 than from normal hearts despite the similar contents of NCX1 and calcineurin in these preparations (Fig. 2*b*).

Interestingly, calmodulin also was more abundant in the immunoprecipitates from BIO14.6 heart, although total calmodulin was again not different (Fig. 2*b*), suggesting that calcineurin is activated in the BIO14.6 heart. Immunocytochemistry with anti-CnAβ revealed the presence of calcineurin at the peripheral sarcolemma in BIO14.6 but not in normal cardiomyocytes, although it was detectable in the cell interior and at the intercalated discs in both types of myocytes (Fig. 2*a*). Striated patterns seen in the cell interior may reflect the presence of calcineurin in the Z-lines (16). Furthermore, calcineurin was more abundant in the membrane *versus* the cytosolic fraction prepared from the BIO14.6 heart, whereas the opposite was true of normal heart muscle (Fig. 2*c*). Thus, the association of calcineurin with NCX1 is significantly enhanced in BIO14.6 compared with normal hearts.

NCX Activity Is Regulated by Calcineurin in Rat Cardiomyocytes or CCL39 Cells Expressing Cloned NCX1—To examine the possible effects of calcineurin on NCX activity, we used rat neonatal cardiomyocytes subjected to pretreatment with 10 μM PE for 72 h (see protocol in Fig. 3*a*). In these myocytes, a prominent increase in cell size with enhanced sarcomere organization and enhanced expression of ANP was observed (Fig. 3*b*) (14, 17, 28). The NCX1 protein was detectable in the sarcolemma, particularly in the intercellular junctions (Fig. 3, *b* and *c*), and its expression greatly increased during the PE treatment, although calcineurin expression remained essentially unchanged (Fig. 3*d*, *top*). We observed overlapping localization of NCX1 and calcineurin in the sarcolemma of myocytes after a 72-h PE treatment, consistent with the finding that a much larger amount of NCX1 protein was recovered in the anti-CnA immunoprecipitates from the PE-treated *versus* non-treated myocytes (Fig. 3*c*). These myocytes did not show a sign of apoptosis, because the number of TUNEL-positive cells was <3% the amount in non-treated control myocytes. Importantly, the rate of Na^+_i-dependent $^{45}Ca^{2+}$ uptake measured as activity per milligram of cell protein was markedly decreased in myocytes after a 72-h PE treatment (Fig. 3*d*, *bottom*). The uptake rate in the latter myocytes would be even smaller if it was normalized to cell NCX1 content (see above). On the other hand, the uptake rate was modestly increased in myocytes after a 24-h PE treatment. This uptake increase may be attributable to the increased NCX1 expression seen at this time point (Fig. 3*d*, *top*).

Intriguingly, when myocytes were treated with 0.01–1 μM the calcineurin inhibitor FK506 during the last 15–30 min of the 72-h PE treatment, the rate of Na^+_i-dependent $^{45}Ca^{2+}$ uptake increased 2-fold (Fig. 4*a*). Qualitatively similar results were obtained with myocytes pretreated with 10% FCS (Fig. 4*a*). Of note, the rate of Na^+_i-dependent $^{45}Ca^{2+}$ uptake also increased by 188 ± 3% (n = 3) when 10 μM cyclosporin A, another calcineurin inhibitor, was added to the PE-treated myocytes. On the other hand, FK506 also enhanced the rate of Na^+_o-dependent Ca^{2+} efflux from PE-pretreated cardiomyocytes (Fig. 4*b*). In this experiment, we loaded PE-treated and non-treated myocytes with $^{45}Ca^{2+}$ to equivalent levels of radioactivity, and $^{45}Ca^{2+}$ efflux was then initiated by acutely raising $[Ca^{2+}]_i$ with thapsigargin under physiological ionic conditions. These data indicate that PE and FK506 regulate both the influx and efflux modes of NCX activity.

To confirm the involvement of calcineurin in NCX regulation, we tested the effect of the adenoviral infection of dominant negative or activated CnA on cardiomyocytes pretreated with PE or FCS for up to 96 h (see Fig. 3*a*). Like FK506, dominant negative CnA, when infected at 72 h after the start of PE treatment, caused a large increase in the rate of Na^+_i-dependent $^{45}Ca^{2+}$ uptake without an appreciable change in the size of the hypertrophic myocytes (Fig. 5). On the other hand, when infected at 24 h after the start of the 72-h PE or FCS treatment, dominant negative CnA nearly prevented the occurrence of the PE- and FCS-induced uptake inhibition and severely depressed myocyte enlargement, whereas it exerted no effects on controls not pretreated with growth factors (Fig. 5 and data not shown). Under similar conditions, activated CnA significantly increased the size of control myocytes as reported previously (28, 29) and reduced the uptake rate in these cells by ~40% (Fig. 5). Furthermore, activated CnA promoted the FCS-induced uptake inhibition, although it exerted little additional effect on PE-treated myocytes. Thus, a significant portion of NCX inhibition occurring in PE- or FCS-pretreated myocytes is due to the enzymic activity of calcineurin.

We next examined the effects of protein kinase modulators on the rate of Na^+_i-dependent Ca^{2+} uptake in chronically PE-treated myocytes. Incubation of myocytes with 0.3 μM PMA during the last 30 min of a 72-h PE treatment caused little effect on the uptake rate (Fig. 6), whereas it produced a 20–30% increase in non PE-pretreated controls (data not shown), consistent with a previous report (9). In contrast, incubation with PMA during the final 24 h of a 72-h PE treatment caused an increase in the uptake rate similar to that seen at 1 μM FK506. The latter PMA effect (PKC down-regulation) was mimicked by a 30-min treatments with PKC inhibitors; the uptake rate in the presence of 0.3 μM calphostin C (Fig. 6), 50

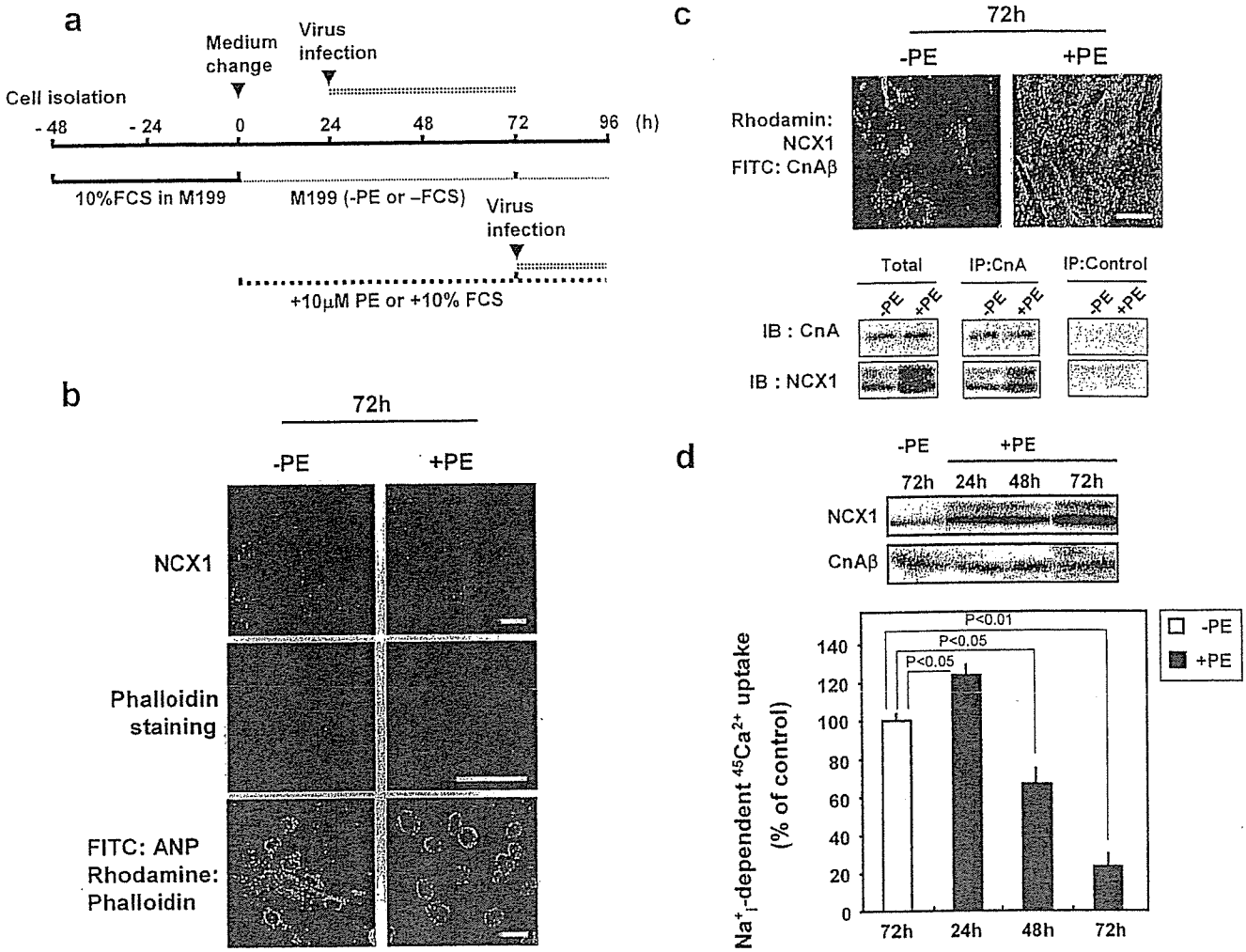

FIG. 3. **Effects of PE treatment on morphology, NCX1 and calcineurin expressions, and Na^+_i-dependent $^{45}Ca^{2+}$ uptake in cardiomyocytes.** *a*, protocol for the treatment of cardiomyocytes with PE and other agents. *b*, characterization of cardiomyocytes after a 72-h treatment with 0 (*−PE*) or 10 μM (*+PE*) PE. *Bar*, 20 μm. *Top*, immunostaining with anti-NCX1; *middle*, sarcomere assembly of myocytes visualized with rhodamine-phalloidin; *bottom*, immunostaining of myocytes with anti-ANP (*green*) and rhodamine-phalloidin (*red*). *FITC*, fluorescein isothiocyanate. *c*, co-localization and association of NCX1 and calcineurin in cardiomyocytes pretreated with PE for 72 h. *Top*, images of PE-treated or non-treated myocytes double-stained with anti-NCX1 (*red*) and anti-CnAβ (*green*). Overlapping stain is shown by *yellow* and *orange colors*. *Bar*, 20 μm. *Bottom*, lysates of PE-treated and non-treated myocytes (*Total*) and materials immunoprecipitated with anti-pan CnA (*IP:CnA*) or no antibody (*IP:control*) were subjected to immunoblot (*IB*) assay with anti-NCX1 or anti-pan CnA. *d*, time-dependent changes in the expression of NCX1 and CnAβ and the rate of Na^+_i-dependent $^{45}Ca^{2+}$ uptake (average ± S.D.; $n = 3$) in cardiomyocytes during treatment with 0 or 10 μM PE.

nM GF109203X, or 1 μM chelerythrine increased by 327 ± 4 ($n = 3$), 300 ± 6 ($n = 3$), and 296 ± 5% ($n = 3$), respectively, as compared with that of PE-treated myocytes. The effects of FK506 and 24-h PMA treatment or calphostin C were additive, suggesting that the enzymic activities of calcineurin and PKC contributed independently to the observed reduction of uptake activity in PE-treated myocytes. Under similar conditions, however, the protein kinase A activator 8-bromo-cAMP (100 μM), the protein kinase A inhibitors Rp-8-CPT-cAMPS (100 μM) and H89 (50 μM), the protein kinase G activator 8-bromo-cGMP (100 μM), the protein kinase G activator inhibitor Rp-8-CPT-cGMPS (100 μM), and the calmodulin-dependent protein kinase II inhibitors KN62 (25 μM) and KN93 (25 μM) did not influence the uptake rate (Fig. 6 and data not shown).

Finally, using CCL39 cells expressing NCX1 variants, we examined the possible role of the central cytoplasmic loop of the exchanger in the reversal of NCX inhibition by the inhibitors of calcineurin and PKC. In cells expressing wild-type NCX1 infected with activated CnA for 48 h, the rate of Na^+_i-dependent $^{45}Ca^{2+}$ uptake was 40% lower compared with that for control cells in which expression of activated CnA had been suppressed with DOX (Fig. 7*a*). Importantly, such uptake reduction was reversed by FK506 but significantly promoted by PMA. Thus, uptake inhibitions by calcineurin and PKC were additive in CCL39 cells as in cardiomyocytes. However, in cells expressing an NCX1 mutant lacking most of its central loop (NCX1Δ246–672), the uptake rate was not affected by either FK506 or PMA (Fig. 7*a*), indicating that the central loop is required for the effects of calcineurin and PKC.

We then used CCL39 cells not infected with activated CnA to examine the possible interaction of endogenous calcineurin with the β1 repeat deletion mutant (NCX1Δ407–478). In one series, thapsigargin was added to cells 30 min before the uptake measurement to induce a low but sustained $[Ca^{2+}]_i$ increase by reducing the Ca^{2+}-buffering capacity of the endoplasmic reticulum and, thus, activate endogenous calcineurin (Fig. 7*b*), whereas it was not added in another series (Fig. 7*c*). The rate of Na^+_i-dependent $^{45}Ca^{2+}$ uptake in cells expressing wild-type NCX1 was ~50 and 20% higher with 1 μM FK506 in thapsigargin-treated and non-treated cells, respectively, compared with those in the absence of FK506. In contrast, FK506 produced little effect on cells expressing either NCX1Δ407–478

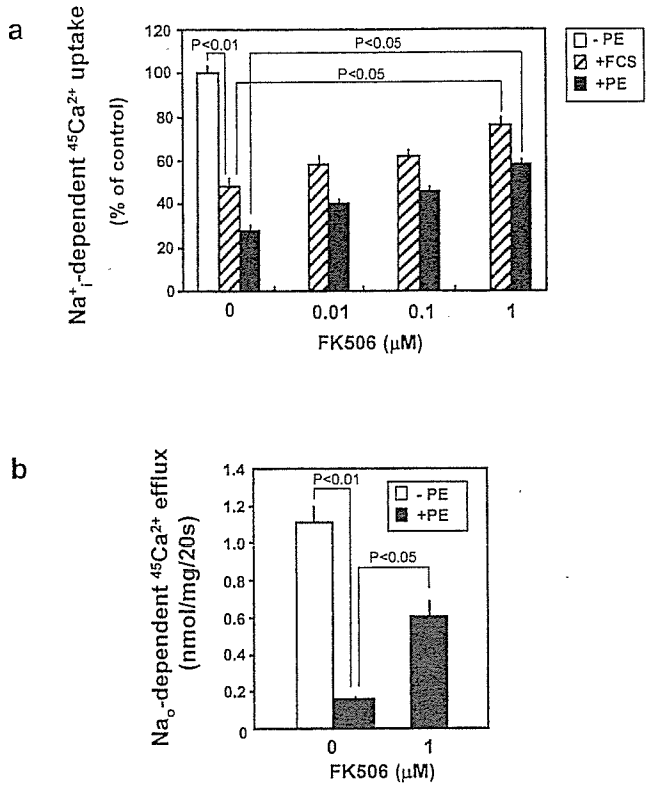

FIG. 4. **Effects of FK506 on Na^+_i-dependent $^{45}Ca^{2+}$ uptake into and Na^+_o-dependent $^{45}Ca^{2+}$ efflux from cardiomyocytes pretreated with PE or FCS.** *a*, myocytes treated with 0 or 10 μM PE or 10% FCS for 72 h (see Fig. 3*a*) were incubated with FK506 for 30 min, and the rates of Na^+_i-dependent $^{45}Ca^{2+}$ uptake were measured. *b*, myocytes were pretreated with PE and FK506 as for *panel a*, and the effect of FK506 on Na^+_o-dependent $^{45}Ca^{2+}$ efflux from PE-treated or non-treated cardiomyocytes were measured. Data in each panel are averages ± S.D. (n = 3).

or NCX1Δ246–672, regardless of thapsigargin treatment (Fig. 7, *b* and *c*). These effects of 1 μM FK506 on NCX activity were significant, suggesting that the β1 repeat is required for the action of endogenous calcineurin.

DISCUSSION

Regulation of Cardiac NCX Activity by Calcineurin and PKC—Recent studies have demonstrated that of the three CnA isoforms, CnAα and CnAβ are expressed in cardiomyocytes, with the latter playing a pivotal role in the induction of cardiac hypertrophy (28, 30). Here, we have provided evidence that the carboxyl tail of CnAβ containing an autoinhibitory domain binds to the β1 repeat of NCX1, one of two internal repeat motifs conserved in the central cytoplasmic loop of NCX family members (31). The β1 repeat constitutes part of the putative Ca^{2+} regulatory site that is responsible for the allosteric regulation of NCX activity by intracellular Ca^{2+} (see review, Ref. 3). Hence, CnAβ binds to a critically important portion of the exchanger. Interestingly, the association of the two proteins was much enhanced in BIO14.6 cardiomyopathic hamster heart (Fig. 2). Furthermore, enhanced association of calcineurin with calmodulin was also observed, suggesting that calcineurin is activated due to a sustained increase in $[Ca^{2+}]_i$ in BIO14.6 cardiomyocytes. Such an interpretation is consistent with our recent report (27).

We used neonatal rat cardiomyocytes treated with 10 μM PE or 10% FCS for 72 h as an *in vitro* hypertrophic model (see Fig. 3*a*). The PE-treated myocytes exhibited typical hypertrophic responses characterized by increased cell size, enhanced sarcomeric organization, and increased ANP expression, although FCS treatment induced less prominent responses (Fig. 3*b*).[2] Importantly, the NCX activity in these hypertrophic myocytes, which was measured as the rate of Na^+_i-dependent $^{45}Ca^{2+}$ uptake or the rate of Na^+_o-dependent Ca^{2+} efflux, was markedly decreased relative to those in non-treated controls (Figs. 3*d* and 4*b*). Such depressed activity was partially reversed by FK506, cyclosporin A, or infection with dominant negative CnA (Figs. 4–6 and "Results"). On the other hand, activated CnA caused a significant decrease in NCX activity in non-treated controls or FCS-treated myocytes, although it had little additional effect on PE-treated cells (Fig. 5). Dominant negative CnA nearly prevented the occurrence of both NCX inhibition and cell hypertrophy in PE- or FCS-treated myocytes (Fig. 5 and "Results"). Therefore, we suggest that calcineurin activity is elevated in PE-treated hypertrophic myocytes as reported previously (28) and that this activity causes NCX inhibition.

PKC inhibitors also caused a partial reversal of depressed NCX activity in PE-treated myocytes (Fig. 6 and "Results"). The effects of the inhibitors of calcineurin and PKC were additive, suggesting that the actions of these enzymes are mutually independent. Importantly, FK506 and calphostin C acted acutely with little influence on myocyte hypertrophic phenotypes. Hence, it is likely that these enzyme actions occur via different mechanisms involving distinct substrate proteins. Of note, however, the PKC-dependent NCX inhibition requires prior activation of calcineurin, because prior infection with dominant negative CnA nearly abolished the PE-induced NCX inhibition (Fig. 5) and because the PKC-dependent NCX inhibition occurred only after the infection of CCL39 cells with activated CnA (Fig. 7*a*).[2] Recent studies (29, 32) have revealed that hypertrophic calcineurin signaling is closely interconnected with activations of PKCα and θ and that PKCα is a necessary mediator of the PE-induced hypertrophy of isolated rat and mouse cardiomyocytes.

The NCX inhibition by calcineurin and PKC seen in PE-treated cardiomyocytes was reproduced in CCL39 cells expressing cloned wild-type NCX1, but not in those expressing NCX1Δ246–672 (Fig. 7*a*), suggesting that the central cytoplasmic loop of NCX1 is required for the effects of calcineurin and PKC. Importantly, this same finding strongly argues against the view that the observed NCX inhibition arose secondarily from changes in cellular conditions, such as altered ion distribution across the plasma membrane. We thus consider that PE alters the functional state of the exchanger causing NCX inhibition. This inhibitory effect of PE, together with the acute NCX stimulation by PE or other agonists of Gαq-coupled receptors reported earlier (8–10), suggests that there exists complex regulatory mechanism(s) for cardiac NCX1.

We observed that the β1 repeat deletion from NCX1 expressed in CCL39 cells abolished the effect of endogenous calcineurin, whereas the deletion of the large cytoplasmic loop abolished the actions of both endogenous calcineurin and recombinant activated CnA (Fig. 7, *a–c*). These data are consistent with the view that NCX1 binding is necessary for the effect of endogenous calcineurin. We speculate that the large cytoplasmic loop of NCX1 may be required to maintain the interaction of calcineurin with its substrate(s). The phosphorylated residues in the cytoplasmic loop might serve as the calcineurin substrate or, alternatively, the cytoplasmic loop could function as a scaffold for ancillary protein(s) that might serve as the substrate. These substrates might be available for the endogenous calcineurin bound to the β1 repeat as well as for the

[2] Y. Katanosaka, S. Wakabaysashi, and M. Shigekawa, unpublished observation.

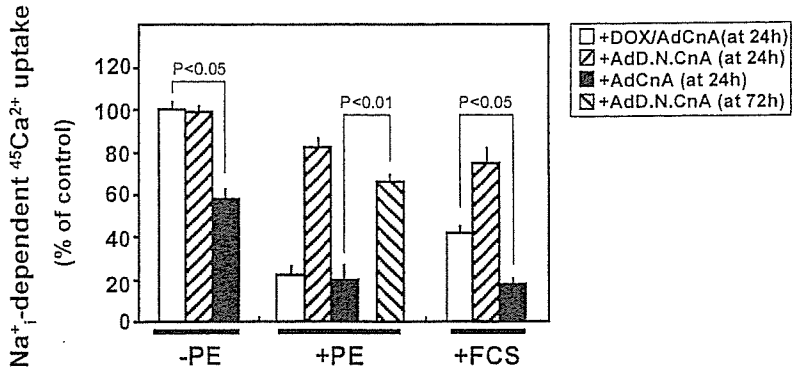

FIG. 5. **Effect of activated or dominant negative CnA on Na^+_i-dependent $^{45}Ca^{2+}$ uptake in cardiomyocytes pretreated with PE or FCS.** Myocytes were treated with no growth factor (*−PE*), 10 μM PE (*+PE*), or 10% FCS (*+FCS*) for 72 h. In one series (*bar* on the *extreme right* for *+PE*), PE-treated myocytes were subsequently infected with dominant negative can, and the rate of Na^+_i-dependent $^{45}Ca^{2+}$ uptake was measured 24 h later. In all other series, myocytes were infected at 24 h after the start of growth factor treatment either with activated CnA in presence (*+DOX/AdCnA*) or absence (*+AdCnA*) of DOX or with dominant negative CnA (*+AdD.N.CnA*), and uptake rates were measured 48 h later. The uptake rate in the *−PE+DOX/AdCnA* series was taken as 100%. Data are averages ± S.D. (n = 3).

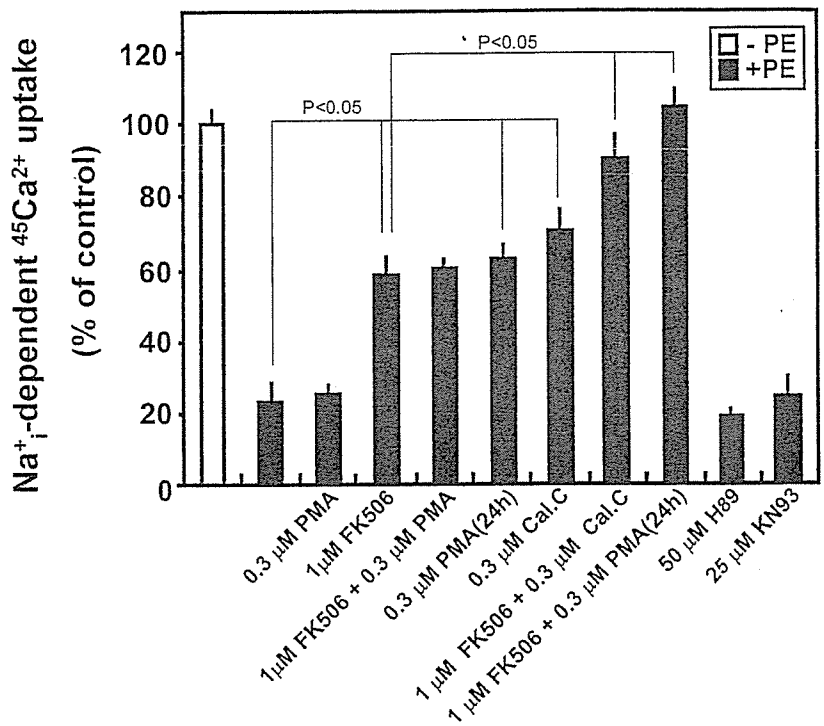

FIG. 6. **Effects of FK506, protein kinase modulators and their combinations on Na^+_i-dependent $^{45}Ca^{2+}$ uptake into PE-treated cardiomyocytes.** Myocytes were incubated with the indicated agents during the last 30 min of a 72-h treatment with 0 or 10 μM PE, and then the rates of Na^+_i-dependent $^{45}Ca^{2+}$ uptake were measured. In some series, myocytes were incubated with 0.3 μM PMA during the last 24 h of PE treatment (*PMA(24h)*). *Cal.C*, calphostin C. Data are averages ± S.D. (n = 3).

recombinant activated CnA overexpressed in myocytes, although this may not happen when the large cytoplasmic loop is deleted. It is noteworthy, however, that activated CnA, lacking its C-terminal tail and the ability to bind to the NCX1 β1 repeat, was able to regulate NCX activity (Fig. 5). Thus, in view of the limitations inherent in these mutation studies, we cannot rule out the possibility that calcineurin may inhibit NCX activity without binding to NCX1. Further studies are required to establish the causal relationship between calcineurin binding and NCX inhibition.

Pathological Relevance of Depressed NCX Function—Myocardial hypertrophy occurs in response to a variety of stimuli, including the chronic activation of $G\alpha^q$ class of G-proteins that leads to the activation of calcineurin, PKC, and mitogen-activated protein kinases (15). On the other hand, calcineurin and its primary downstream effector, the nuclear factor of activated T cells (NFAT), have been shown to be important mediators of *in vitro* and *in vivo* cardiac hypertrophic responses (see reviews, Refs. 15 and 16). The exact mechanism by which calcineurin promotes pathological hypertrophic responses is currently unknown, as few targets for calcineurin other than the NFATs that contribute to the development of cardiac hypertrophy have been identified. This study has provided evidence suggesting that NCX1 may be one of such targets for calcineurin. The results shown here are in good agreement with the recent report by Wang *et al.* (33) showing that NCX current density was significantly reduced in hypertrophic cardiomyocytes isolated from aortic banded mice, whereas this did not occur in mice receiving daily cyclosporin A injection during aortic constriction. Because depressed NCX activity is likely to cause the chronic elevation of $[Ca^{2+}]_i$ in cardiomyocytes, depressed NCX activity might play an important role in the development of myocardial hypertrophy and the subsequent contractile dysfunction. However, the pathological significance of depressed NCX activity needs to be established in future studies, as enhanced NCX1 expression and function have also

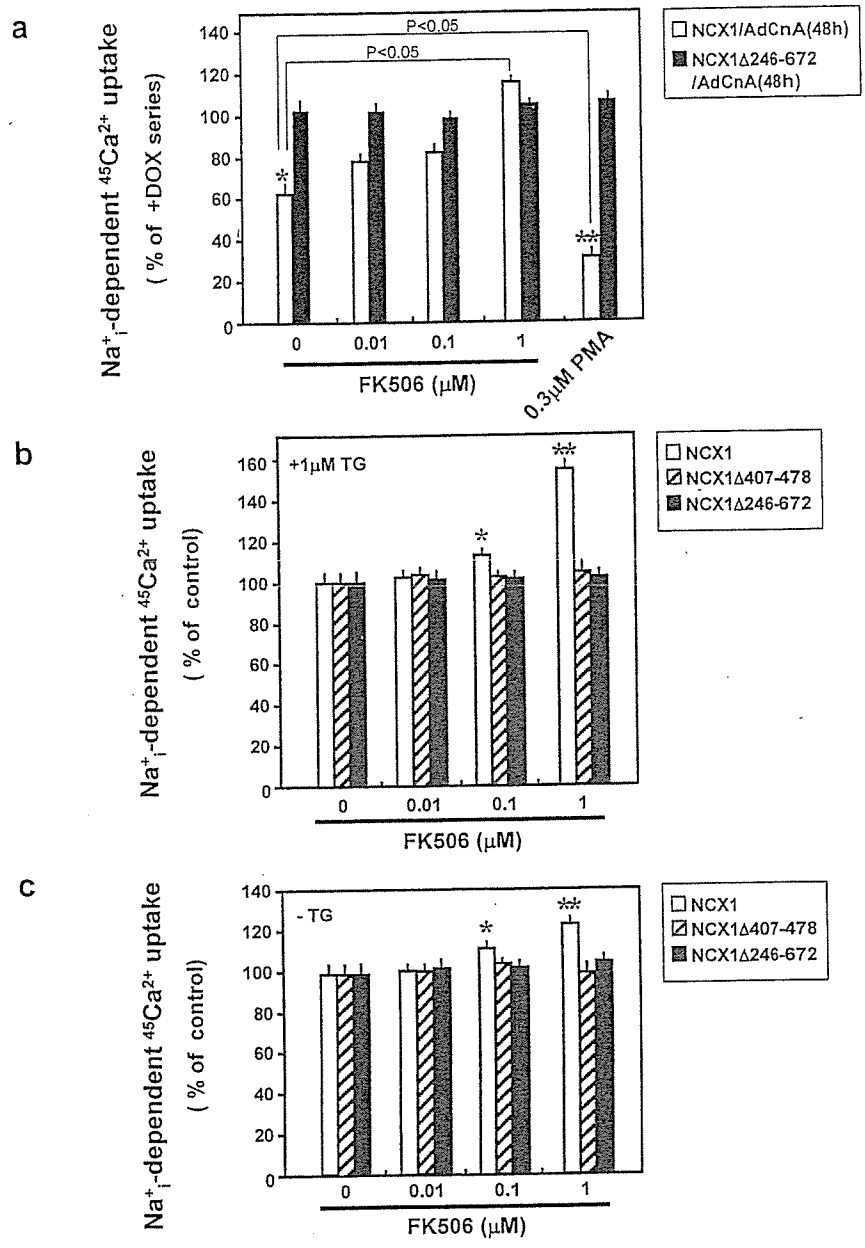

FIG. 7. **Effect of FK506 or PMA on Na^+_i-dependent $^{45}Ca^{2+}$ uptake into CCL39 cells expressing NCX1 variants and/or activated CnA.** *a*, cells expressing wild-type NCX1 or NCX1Δ246–672 were infected with activated CnA (*AdCnA*) for 48 h in the presence or absence of 1 μM DOX. The cells were then incubated with the indicated concentrations of FK506 or PMA for 30 min, and the rates of Na^+_i-dependent $^{45}Ca^{2+}$ uptake were measured. The uptake rate in the series with activated CnA in the presence of DOX (+DOX/AdCnA) was taken as 100%. *b*, cells expressing wild-type NCX1, NCX1Δ407–478, or NCX1Δ246–672 were incubated with 1 μM thapsigargin (*TG*) and the indicated concentrations of FK506 for 30 min, and the uptake rates were measured. *c*, the uptake rate was measured as for *panel b*, except that thapsigargin was omitted. In *panels b* and *c* the uptake rate with no FK506 was taken as 100% for each NCX variant. Data are averages ± S.D. ($n = 9$). *, $p < 0.05$ *versus* control; **, $p < 0.01$ *versus* control.

been reported for cardiomyocytes isolated from some animal models of cardiac hypertrophy and heart failure (6, 7).

REFERENCES

1. Bridge, J. H. B., Smolley, J. R., and Spitzer, K. W. (1990) *Science* 248, 376–378
2. Bers, D. M. (2000) *Circ. Res.* 87, 275–281
3. Shigekawa, M., and Iwamoto, T. (2001) *Circ. Res.* 88, 864–876
4. Kent, R. L., Rozich, J. D., McCollam, P. L., McDemott, D. E., Thacker, U. F., Menick, D. R., McDermott, P. J., and Cooper, G., IV (1993) *Am. J. Physiol.* 265, H1024–H1029
5. Studer, R., Reinecke, H., Biger, J., Eschenhagen, T., Böhm, M., Hasenfuss, G., Just, H., Holtz, J., and Drexler, H. (1994) *Circ. Res.* 75, 443–453
6. Ahmmed, G. U., Dong, P. E., Song, G., Ball, N. A., Xu, Y., Walsh, R. A., and Chiamvimonvat, N. (2000) *Circ. Res.* 86, 558–570
7. O'Rourke, B., Kass, D. A., Tomaselli, G. F., Kääb, S., Tunin, R., and Marbán, E. (1999) *Circ. Res.* 6, 558–570
8. Iwamoto, T., Pan, Y., Wakabayashi, S., Imagawa, T., Yamanaka, H. I., and Shigekawa, M. (1996) *J. Biol. Chem.* 271, 13609–13615
9. Iwamoto, T., Pan Y., Nakamura, T. Y., Wakabayashi, S., and Shigekawa, M. (1998) *Biochemistry* 37, 17230–17238
10. Stengl, M., Mubagwa, K., Carmeliet, E., and Flameng, W. (1998) *Cardiovasc. Res.* 38, 703–710
11. Link, B., Qiu, Z., He, Z., Tong, Q., Hilgemann, D.W., and Philipson, K.D. (1998) *Am. J. Physiol.* 274, C415–C423
12. Wei, S.-K., Ruknudin, A., Hanlon, S. U., McCurley, J. M., Schulze, D. H., and Haigney, M. C. P. (2003) *Circ. Res.* 92, 897–903
13. Condrescu, M., Hantash, B. M., Fang, Y., and Reeves, J. P. (1999) *J. Biol. Chem.* 274, 33279–33286
14. Molkentin, J. D., Lu, J.-R., Antos, C. L., Markham, B., Richardson, J., Robins, J., Grant, S. R., and Olson, E. N. (1998) *Cell* 93, 215–228
15. Molkentin, J. D., and Dorn, G. W., II (2001) *Ann. Rev. Physiol.* 63, 391–426
16. Vega, R. B., Bassel-Duby, R., and Olson, E. N. (2003) *J. Biol. Chem.* 278, 36981–36984
17. Simpson, P., McGrath, A., and Savion, S. (1982) *Circ. Res.* 51, 787–801
18. Shibasaki, F., and MacKeon, F. (1995) *J. Cell Biol.* 131, 735–743
19. Wang, H.-G., Pathan, N., Ethell, I. M., Krajewski, S., Yamaguchi, Y., Shibasaki, F., Mckeon, F., Bobo, T., Franke, T. F., and Reed, J. C. (1999) *Science* 284, 339–343
20. Laemmli, U. K. (1970) *Nature* 227, 680–685
21. Tawada-Iwata, Y., Imagawa, T., Yoshida, A., Takahashi, M., Nakamura, H., and Shigekawa, M. (1993) *Am. J. Physiol.* 264, H1447–H1453
22. Pan ,Y., Iwamoto, T., Uehara, A., Nakamura, T. Y., Imanaga, I., and Shigekawa, M. (2000) *Am. J. Physiol.* 279, C393–C402
23. Furukawa, K., Tawada, Y., and Shigekawa, M. (1988) *J. Biol. Chem.* 263, 8058–8065
24. Saito, S., Hiroi, Y., Zou, Y., Aikawa, R., Toko, H., Shibasaki, F., Yazaki, Y., Nagai, R., and Komuro, I. (2000) *J. Biol. Chem.* 275, 34528–34533
25. Bajusz, E., Homburger, F., Baker, J. R., and Bogdonoff, P. (1969) *Ann. N. Y. Acad. Sci.* 156, 396–420
26. Nigro, V., Okazaki, Y., Belsito, A., Piluso, G., Matsuda, Y., Politano, L., Nigro, G., Ventura, C., Abbondanza, C., Molinari, A. M., Acampora, D., Nishimura,